Heliyon 10 (2024) e28936

Contents lists available at ScienceDirect

Heliyon

journal homepage: www.cell.com/heliyon

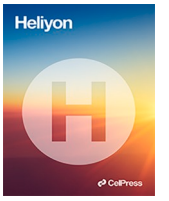

Research article

$PM_{2.5}$, component cause of severe metabolically abnormal obesity: An in silico, observational and analytical study

Sagrario Lobato [a,b,c,*], A. Lourdes Castillo-Granada [c,d], Marcos Bucio-Pacheco [c,e], Víctor Manuel Salomón-Soto [c], Ramiro Álvarez-Valenzuela [c], Perla Margarita Meza-Inostroza [c], Raúl Villegas-Vizcaíno [c]

[a] *Departamento de Investigación en Salud, Servicios de Salud del Estado de Puebla, 15 South Street 302, Puebla, Mexico*
[b] *Promoción y Educación para la Salud, Universidad Abierta y a Distancia de México. Universidad Avenue 1200, 1st Floor, quadrant 1-2, Xoco, Benito Juarez, 03330, Mexico City, Mexico*
[c] *Educación Superior, Centro de Estudios, "Justo Sierra", Surutato, Badiraguato, Mexico*
[d] *Facultad de Estudios Superiores Zaragoza, Universidad Nacional Autónoma de México, Guelatao Avenue 66, Ejército de Oriente Indeco II ISSSTE, Iztapalapa, 09230, Mexico City, Mexico*
[e] *Facultad de Biología, Universidad Autónoma de Sinaloa, Americas Avenue, Universitarios Blvd., University City, 80040, Culiacán Rosales, Mexico*

ARTICLE INFO

Keywords:
Metabolically abnormal obesity
Airborne particulate matter
Causality
Transcriptional signatures

ABSTRACT

Obesity is currently one of the most alarming pathological conditions due to the progressive increase in its prevalence. In the last decade, it has been associated with fine particulate matter suspended in the air ($PM_{2.5}$). The purpose of this study was to explore the mechanistic interaction of $PM_{2.5}$ with a high-fat diet (HFD) through the differential regulation of transcriptional signatures, aiming to identify the association of these particles with metabolically abnormal obesity. The research design was observational, using bioinformatic methods and an explanatory approach based on Rothman's causal model. We propose three new transcriptional signatures in murine adipose tissue. The sum of transcriptional differences between the group exposed to an HFD and $PM_{2.5}$, compared to the control group, were 0.851, 0.265, and −0.047 ($p > 0.05$). The HFD group increased body mass by 20% with two positive biomarkers of metabolic impact. The group exposed to $PM_{2.5}$ maintained a similar weight to the control group but exhibited three positive biomarkers. Enriched biological pathways ($p < 0.05$) included PPAR signaling, small molecule transport, adipogenesis genes, cytokine-cytokine receptor interaction, and HIF-1 signaling. Transcriptional regulation predictions revealed CpG islands and common transcription factors. We propose three new transcriptional signatures: FAT-$PM_{2.5}$-CEJUS, FAT-$PM_{2.5}$-UP, and FAT-$PM_{2.5}$-DN, whose transcriptional regulation profile in adipocytes was statistically similar by dietary intake and HFD and exposure to $PM_{2.5}$ in mice; suggesting a mechanistic interaction between both factors. However, HFD-exposed murines developed moderate metabolically abnormal obesity, and $PM_{2.5}$-exposed murines developed severe abnormal metabolism without obesity. Therefore, in Rothman's terms, it is concluded that HFD is a sufficient cause of the development of obesity, and $PM_{2.5}$ is a component cause of severe abnormal metabolism of obesity. These signatures would be integrated into a systemic biological process that would induce transcriptional regulation in trans, activating obesogenic biological pathways, restricting

* Corresponding author. Head of Departamento de Investigación en Salud, Servicios de Salud del Estado de Puebla, 15 South Street 302, Puebla, Mexico.
E-mail address: sagrariolobato@cejus.edu.mx (S. Lobato).

https://doi.org/10.1016/j.heliyon.2024.e28936
Received 23 January 2024; Received in revised form 26 March 2024; Accepted 27 March 2024
Available online 3 April 2024

lipid mobilization pathways, decreasing adaptive thermogenesis and angiogenesis, and altering vascular tone thus inducing a severe metabolically abnormal obesity.

Abbreviations

BAT	brown adipose tissue
BH	Benjamin & Hochberg method
BMI	Body Mass Index
CGI	CpG islands
CTD	Comparative Toxicogenomics Database
FDR	false discovery rate
GEO	Gene Expression Omnibus
GSEA	gene set enrichment analysis
HFD	high-fat diet
HIF-1	hypoxia-inducible factor-1
Inr	initiator element
Log_2FC	logarithm base 2 of Fold Change
LPL	lipoprotein lipase
MEME	suite Multiple Expectation Maximization for Motif Elicitation
NCBI	National Center for Biotechnology Information
ORA	Over-Representation Analysis
$PM_{2.5}$	fine particulate matter suspended in the air with a diameter $\leq$2.5 μm
PPAR	peroxisome proliferator-activated receptors
ROS	reactive oxygen species
TG	triglycerides
TF	transcription factor
TPM	transcripts per million
UCP1	uncoupling protein 1
WAT	white adipose tissue
WebGestalt	WEB-based GEne SeT AnaLysis Toolkit
WHO	World Health Organization

1. Introduction

Obesity is currently one of the most alarming pathological conditions, with its prevalence consistently increasing globally over the past five decades [1,2]. Defined as a multifactorial disease [3,4], it involves the excessive accumulation of body fat beyond physiological needs and adaptive capacity, leading to adverse health consequences [5,6]. There are two ways to classify this disease. On one hand, the World Health Organization (WHO) classifies it as Class I when the Body Mass Index (BMI) is 30–34.9 kg/m^2, Class II when the BMI is 35–39.9 kg/m^2, and Class III or severe, extreme, or massive obesity when the BMI is $\geq$ 40 kg/m^2 [7,8]. A second classification is based on the accompanying metabolic alterations, including metabolically healthy obesity, metabolically abnormal obesity [9,10], and obesity with sarcopenia [11].

In the last decade, environmental pollution has been suggested as a multifactorial contributor to obesity following the identification of correlations between the two [12,13]. Population growth, the economy reliant on fossil fuels, and natural sources of particulate matter have elevated air pollution worldwide to unprecedented levels [14,15]. To such an extent, in 2021, the World Health Organization declared it the most significant environmental health concern [16]. One of these pollutants is fine particulate matter suspended in the air with a diameter of $\leq$2.5 μm ($PM_{2.5}$) [16,17].

Recent reports indicate that over 90% of the global population is exposed to $PM_{2.5}$ concentrations exceeding the guideline set by the WHO of 5 $\mu g/m^3$ annually [16,18]. Experimental studies have been published, and their results indicate gene regulation disruption following exposure to $PM_{2.5}$ [19,20]. An increase in the expression of the *Ucp1* gene has been observed in brown adipose tissue of mice exposed to these particles, along with alterations in the leptin signaling pathway, among other findings. The conclusion is that prolonged exposure to $PM_{2.5}$ induces leptin resistance, hyperphagia, and a in decreased energy expenditure [21].

While the scientific community acknowledges the multifactorial etiology of obesity, discrepancies persist in the weighting of etiological factors contributing to the rise of this disease [22]. The inconsistencies could be attributed to the dominant model of causality in epidemiology, the Bradford-Hill model [23–26], which, although it identifies the etiological factors, limits the estimation of the type of cause and its weight in the etiology of the disease. In 1976, Rothman [27] proposed an alternative model that addresses this limitation, bridging the gap between the metaphysical notions of cause and fundamental epidemiological parameters [28]. He

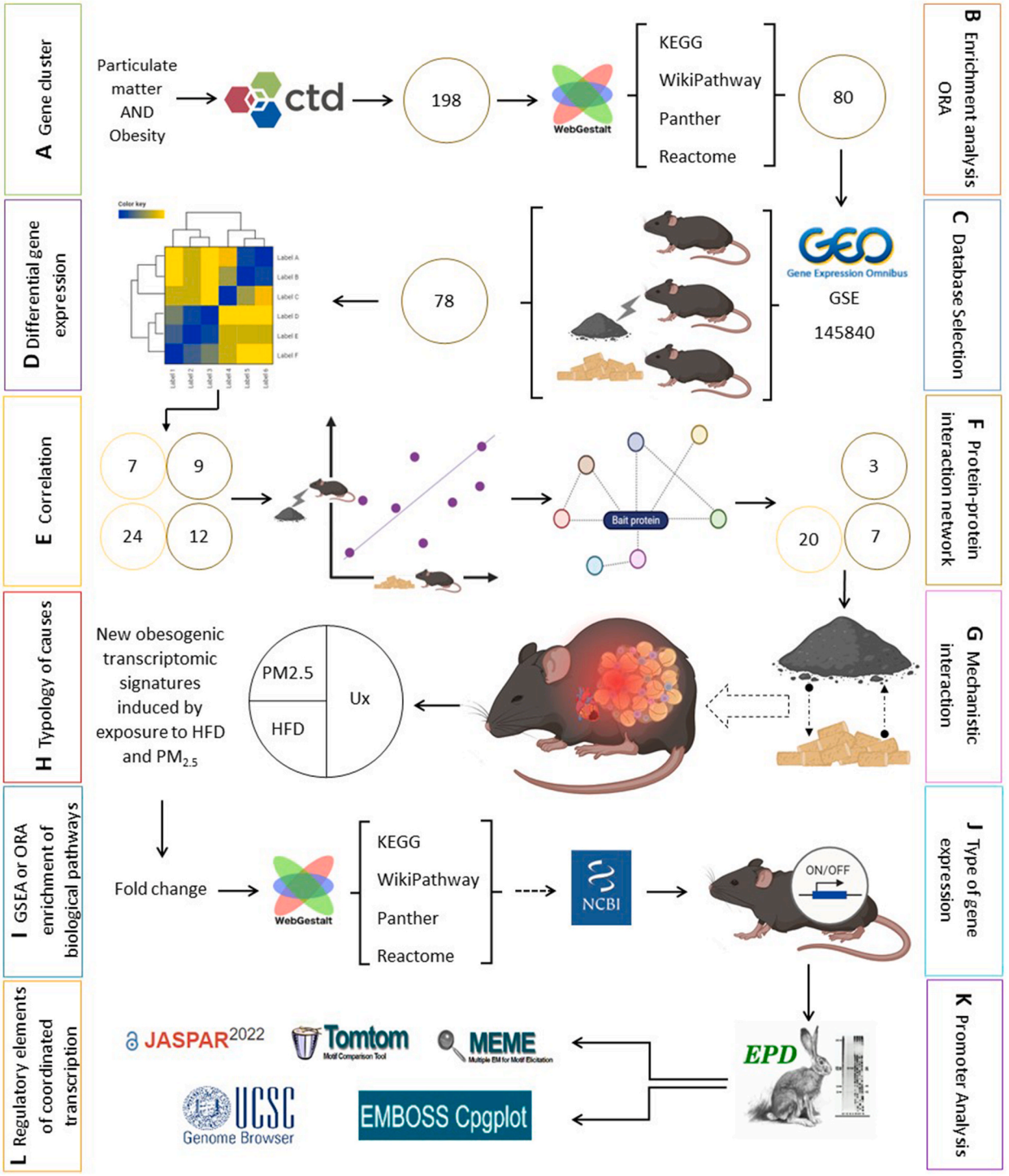

(caption on next page)

Fig. 1. Methodological strategy
A. Initial cluster of genes associated with obesity and particulate matter in the Comparative Toxicogenomics Database (CTD). B. The genes underwent Overrepresentation Enrichment Analysis (ORA) on the WEB-based GEne SeT AnaLysis Toolkit (WebGestalt) platform using the 'KEGG pathway,' 'Wikipathway,' 'Panther,' and 'Reactome' repositories. C. Selection of transcriptome database in the GEO Gene Expression Omnibus database for in silico analysis through cases and controls. D. Analysis of differential gene expression on the Morpheus Broad Institute platform. E. Estimation of Spearman correlation between transcription due to $PM_{2.5}$ exposure and high-fat diet (HFD) intake. F. Biological association through protein-protein interaction networks on the STRING platform. G. Causal inference with the mechanistic interaction of $PM_{2.5}$ with HFD. H. Causal typology with the Rothman model. I. Analysis of biological pathway enrichment on the WebGestalt. J. Identification of gene expression type in the National Center for Biotechnology Information (NCBI). K. Promoter analysis using the Eukaryotic Promoter Database (EPD) platforms. L. Analysis of transcriptional regulatory elements on the Multiple Expectation Maximization for Motif Elicitation (MEME suite), TomTom, JASPAR2022, EMBOSS CpGplot program, and UCSC Genome Browser platforms.

identifies three causes and their relationship with the disease: 1. Sufficient cause constitutes a complete causal mechanism, a minimal set of conditions and events sufficient for the outcome. 2. Component cause can be part of a sufficient cause. 3. Necessary cause is a component cause that complements all sufficient causes [27]. In 2021, Rothman et al. explored the limitations in assessing combined effects in biological processes. Although it can be understood if exposure to two factors causes a result, what he called mechanistic interaction, it is essential to distinguish between mechanistic interaction and biological interaction, as the former does not imply the latter [29].

So, in terms of Rothman,we hypothesize that long-term exposure to $PM_{2.5}$ is not a sufficient cause to produce obesity but rather a component cause. However, these particles may interact with obesogenic factors, enhancing the development of metabolically abnormal obesity by disrupting gene groups in adipocytes. The study's main purpose was to explore the mechanistic interaction [29] of $PM_{2.5}$ with a high-fat diet (HFD) through the differential regulation of transcriptional signatures, aiming to identify the association of these particles with metabolically abnormal obesity. The specific objectives were: 1. To characterize obesogenic transcriptional signatures with abnormal metabolism induced by exposure to HFD and $PM_{2.5}$. 2. To analyze in silico the biological pathways of obesogenic transcriptional signatures with abnormal metabolism induced by exposure to HFD and $PM_{2.5}$. 3. To analyze in silico the promoters of obesogenic transcriptional signatures with abnormal metabolism induced by exposure to HFD and $PM_{2.5}$.

2. Materials and methods

2.1. Study design, data, and variables

The study design was observational, using bioinformatic methods and an explanatory approach based on Rothman's causal model [27,29]. The research was conducted from February to June 2023. The dependent variable was metabolically abnormal obesity, while the independent variables were the intake of an HFD and chronic exposure to $PM_{2.5}$.

2.2. Over-Representation Analysis of genes associated with particulate matter and obesity

The Comparative Toxicogenomics Database (CTD) [30] (Fig. 1A) identified an initial cluster of 198 human genes associated with particulate matter and obesity (see Table S1). This cluster underwent Over-Representation Analysis (ORA) through the WEB-based GEne SeT AnaLysis Toolkit (WebGestalt) platform (http://www.webgestalt.org/) [31], utilizing the 'KEGG pathway,' 'Wikipathway,' 'Panther,' and 'Reactome' repositories (Fig. 1B). We measured the fraction of the 198-gene cluster belonging to the reference gene set, extracted from Illumina humanht-123. Significance was determined with a false discovery rate (FDR) of 0.05, a minimum gene count of five, a maximum gene count of 2000, adjustment using the Benjamin & Hochberg (BH) method, ten expected categories per set, and 40 visualized categories. Obesity-related biological pathways meeting an enrichment ratio $\geq$10 and an FDR $\leq$0.05 were selected (Fig. S1). The resulting 80 genes are detailed in Table S2.

2.3. GEO DataSets selection

The 80 genes were analyzed in silico in the Gene Expression Omnibus (GEO) database (https://www.ncbi.nlm.nih.gov/geo/) [32] (Fig. 1C). The search focused on $PM_{2.5}$, limited to expression profiling by high throughput sequencing, *Mus musculus, Rattus norvegicus*, and transcriptomic profiles in adipocytes. The results underwent content analysis (see Table S3), and only the GSE145840 series by Rajagopalan et al. [33] met the criteria. Raw data were normalized to transcripts per million (TPM), and the median was calculated using the ratios method [34–36].

2.4. Cases and controls

Rajagopalan et al. [33] reported 78 out of the 80 transcripts of interest in nine brown adipose tissue (BAT) samples and eleven white adipose tissue (WAT) samples (78 transcripts x 20 biological samples) from DIO C57BL/6J mice (Fig. 1C). The case and control groups were organized as follows: Cases included three BAT and four WAT samples from mice fed an HFD and exposed to filtered air, along with three BAT and three WAT samples from mice with chronic exposure to $PM_{2.5}$ and fed a regular diet. Controls comprised three BAT and four WAT samples from mice fed a regular diet and exposed to filtered air.

2.5. Differential transcriptional regulation

The transcripts from the cases and control groups were analyzed using the Morpheus Broad Institute program (https://software.broadinstitute.org/morpheus/) (Fig. 1D), using z-score [37–39], hierarchical clustering, and Euclidean distance to identify gene expression regulation, to identify the regulation of gene expression (see Fig. S2). Transcripts with opposite regulation were selected, generating four clusters: two in white adipocytes (one upregulated with seven transcripts and one downregulated with 24) and two in brown adipocytes (one upregulated with nine transcripts and one downregulated with 12) (see Table S4). Transcription values were subjected to the Shapiro-Wilk normality test using SPSS Statistics v29.0 (IBM, NY, USA); the p-value in white and brown adipose tissue under the three conditions was <0.05, proceeding to non-parametric inferential statistics.

2.6. Correlation post-exposure to HFD and $PM_{2.5}$

The four transcript clusters were analyzed using the Spearman correlation coefficient (Fig. 1E) and SPSS Statistics v29.0 (IBM, NY, USA). To avoid statistical artifacts, correlations were also calculated between the transcriptional profile of controls and that of HFD and exposure to $PM_{2.5}$. In both adipose tissues, no significant correlations were observed in the controls, and only one case showed a low inverse correlation (see Table S5).

2.7. Protein-protein interaction network

The four transcript clusters were analyzed using the STRING platform version 11.5 (https://string-db.org/) for protein-protein interaction network analysis [40], with high confidence and a 5% FDR stringency. Genes whose proteins did not show interaction were excluded, resulting in three final clusters (Fig. S3). One in white adipose tissue comprises 20 down-regulated genes, and two in brown adipose tissue, one with three up-regulated genes and another with seven down-regulated genes (Fig. 1F). These three clusters were identified as transcriptional signatures A, B, and C, respectively (see Table S6).

2.8. Rothman's causal model

The resulting transcriptional signatures underwent causality analysis using the Rothman model [27,29] (Fig. 1G). The mechanistic interaction of $PM_{2.5}$ with HFD was assessed through transcriptional differences using the following procedure: 1. Differences between the medians of the transcriptional profile of the HFD-exposed group and the control group were calculated. 2. Similar calculations were performed for the $PM_{2.5}$-exposed group compared to the control group. 3. The interaction between HFD and $PM_{2.5}$ was assessed by calculating the differences between their transcriptional profiles. 4. The differences were summed and compared to analyze the transcriptional similarity to the control group. 5. The procedure was repeated with the genes discarded during the investigation to avoid statistical artifacts. 6. The hypothesis test was applied using the Wilcoxon test for all groups.

To establish the type of causation represented by HFD and exposure to $PM_{2.5}$ in metabolically abnormal obesity (Fig. 1H), the results of body mass and metabolic biomarkers in the mice from Rajagopalan et al. [33] were analyzed. Obesity was defined as a 20–30% increase in body mass compared to controls [41,42], accompanied by $\geq$ two abnormal metabolic parameters in fasting conditions [11,43,44]: insulin resistance [11,45], hypertriglyceridemia [11,46–48], and total hypocholesterolemia [41,49]. The presence of two positive criteria was classified as moderate abnormal metabolism, while three criteria were indicative of severe abnormal metabolism.

Molecular signature repositories and scientific databases were reviewed, and genetic and transcriptional signatures unrelated to genetically originated obesity were selected (see Table S7). The selected signatures were analyzed using a Venn diagram on the Bioinformatics & Evolutionary Genomics platform (https://bioinformatics.psb.ugent.be/webtools/Venn/). A new transcriptional signature was considered when all the genes from each of the three proposed signatures did not overlap with the genes of the reference signatures.

2.9. Enrichment analysis of their biological pathways

The Log_2 Folds Change (Log_2FC) of the three transcriptional signatures from the HFD-exposed group compared to the control group and from the $PM_{2.5}$-exposed group compared to the control group were calculated (Fig. 1I). The Log_2FC of the signatures underwent Gene Set Enrichment Analysis (GSEA) on the WebGestalt platform [31] with the aforementioned repertoires for *Mus musculus*. The analysis used an FDR of 0.05, a minimum of five genes, a maximum of 2000 genes, and 1000 permutations. Signatures without results underwent ORA with previous parameters. Biological pathways with significant enrichment in both enrichment analyses were selected, considering a p-value ≤ 0.05 and FDR ≤ 0.25 [50]. In addition, in the ORA, pathways with the highest number of signature genes corresponding to the abnormal metabolism of the mice and the studied cell type were chosen (see Table S8). The schematics of each pathway were downloaded from biological repositories through the WebGestalt platform [51,52].

2.10. Gene expression type

The summary annotation of each gene of the signatures was reviewed in the National Center for Biotechnology Information (NCBI) (https://www.ncbi.nlm.nih.gov/) (Fig. 1J) selecting the gene of interest from the *Mus musculus* species to identify the type of

expression.

2.11. Identification of promoter regions

The promoter regions of the genes from these signatures were determined in the Eukaryotic Promoter Database (EPD) (http://epd.vital-it.ch) [53] (Fig. 1K). To achieve this, genes were searched for, and their promoter annotations were copied into a table [54,55] from the "General information" section. The NCBI reference sequences of the primary promoters were downloaded in FASTA format (see Table S9). The core region was analyzed for the following elements [56]: the TATA box [57,58], initiator element (Inr) [58,59], Ohler 1 motif [60,61], and the TATA box-like element [62].

2.12. Regulatory elements of coordinated transcription

Primary promoter sequences that did not yield significant results in the biological pathway enrichment analyses were examined using the Multiple Expectation Maximization for Motif Elicitation (MEME suite) version 5.5.2 (https://meme-suite.org/meme/tools/meme) [55] (Fig. 1L), selecting five motifs. Results were opened in MEME HTML format to discover motifs and their locations. Sequences of the motifs and their locations were downloaded in block diagrams. The motifs were subjected to the TomTom platform for comparison with the JASPAR2022_CORE_vertebrates_non-redundant_v2 motif database to determine if a newly discovered putative motif resembled any of the previously discovered regulatory motifs for transcription factors (TFs), using the statistical measure of motif-motif similarity. TFs of the motifs with the lowest E-value were compiled for further analysis [55] (Fig. 1L).

Finally, putative CpG islands (CGI) were searched only in the primary promoter sequences of genes that did not yield significant results in the biological pathway enrichment analyses, predicted using the Takai and Jones algorithm [63] in its modified form: length >200 bp, GC content >50%, and observed CpG/expected CpG >0.60 [55,64]. The EMBOSS CpGplot program (https://www.ebi.ac.uk/Tools/seqstats/emboss_cpgplot/) [59,65] was used for this purpose (Fig. 1L). These putative CGIs were searched in the UCSC Genome Browser (https://genome.ucsc.edu/) [53], selecting the mouse genome GRCm39/m.

3. Results

3.1. $PM_{2.5}$, cofactors for severe metabolically abnormal obesity

Table 1 presents the transcriptional differences induced by a high-fat diet (HFD) and chronic exposure to $PM_{2.5}$. The sum of transcriptional differences in the signatures associated with clusters A, B, and C did not reveal statistically significant differences, contrary to transcriptional differences in the control clusters in white and brown adipose tissues. These results indicate that both HFD and $PM_{2.5}$ exposure affects the transcription of the same genes with similar levels of regulation in clusters A, B, and C, reflecting a mechanistic interaction in the development and severity of obesity.

The metabolic conditions described by Rajagopalan et al. [33] analyzed biological processes underlying the mechanistic interaction. Based on metabolic biomarkers, it was observed that, on average, mice exposed to HFD developed moderately abnormal metabolic obesity (Fig. 2A), whereas mice exposed to $PM_{2.5}$ exhibited severe abnormal metabolism without obesity. According to the Rothman causal model, these results indicate that $PM_{2.5}$ exposure and HFD act as cofactors in developing severe metabolically abnormal obesity, as illustrated in Fig. 2B.

FAT-$PM_{2.5}$-CEJUS, FAT-$PM_{2.5}$-UP, and FAT-$PM_{2.5}$-DN activate obesogenic biological pathways and promote abnormal metabolism.

The confirmation of the in silico discovery of three obesogenic transcriptional signatures with abnormal metabolism induced by exposure to HFD and $PM_{2.5}$ (Table 2) was achieved through comparison with published obesogenic genetic and transcriptional signatures (see Fig. S4). The relationship between the expression changes of the new transcriptional signatures induced by exposure to HFD and $PM_{2.5}$. In both exposures, it was observed that *Ghrl, Ucp1, Apoa1*, and *Apoa5* were the genes with the highest expression change in the FAT-$PM_{2.5}$-CEJUS signature; *Ppara* in the FAT-$PM_{2.5}$-UP signature; and *Prkar1a* and *Il6* in the FAT-$PM_{2.5}$-DN signature (Fig. 3A and Fig. 3B).

Table 1
Sum of transcriptional differences of the new transcriptional signatures and control clusters.

Transcripts	Ctrl (−) HFD	Ctrl (−) $PM_{2.5}$	HFD (−) $PM_{2.5}$
	Median (TPM) of ratios method		
Signature | Cluster A	−3.589	−4.440	0.851*
Signature | Cluster B	0.608	0.343	0.265*
Signature | Cluster C	−10.703	−10.750	−0.047*
Control Cluster | White adipose tissue not considered in clusters A, B, or C	−1.954	0.160	−2.114**
Control Cluster | Brown adipose tissue not considered in clusters A, B, or C	−4.691	1.191	−5.882**

*p > 0·05.
**p < 0·05.
HFD= High-fat diet.
Ctrl = Control.

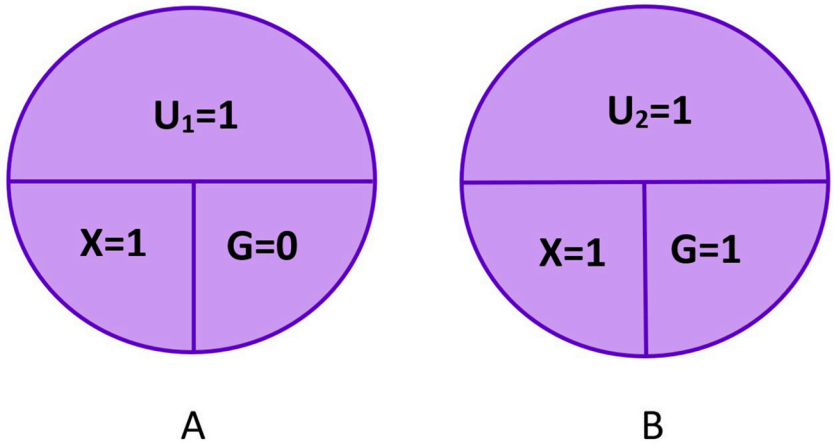

Fig. 2. Two causal models by Rothman
A, obesity model. B, severely metabolically abnormal obesity model. X, exposure to high fat diet (HFD). G, exposure to $PM_{2.5}$. U_1 and U_2 are additional unknown factors to complete sufficient causes. 1, present. 0, absent.

Table 2
New transcriptional signatures.

Contributed by	Sagrario Lobato, with the supervision of Marcos Bucio-Pacheco, A. Lourdes Castillo-Granada, Víctor Manuel Salomón-Soto, Ramiro Álvarez-Valenzuela, Perla Margarita Meza-Inostroza, and Raúl Villegas-Vizcaíno | Centro de Estudios Justo Sierra. Educación Superior. Surutato, Badiraguato, Sinaloa, Mexico.					
Organism	*Mus musculus*					
Standard Name	**FAT-$PM_{2.5}$-CEJUS**		**FAT-$PM_{2.5}$-UP**		**FAT-$PM_{2.5}$-DN**	
Brief Description	Obesogenic transcriptomic signature with severe abnormal metabolism induced by high-fat diet (HFD) and $PM_{2.5}$.					
	The genes composing this signature exhibit a downregulated transcriptional profile in white adipose tissue following exposure to HFD and $PM_{2.5}$		The genes comprising this signature exhibit an upregulated transcriptional profile in brown adipose tissue following exposure to HFD and $PM_{2.5}$		The genes comprising this signature exhibit a downregulated transcriptional profile in brown adipose tissue following exposure to HFD and $PM_{2.5}$.	
Genes	*NCBI (Entrez) Gene Id*	*Symbol*	*NCBI (Entrez) Gene Id*	*Symbol*	*NCBI (Entrez) Gene Id*	*Symbol*
	11364	*Acadm*	12606	*Cebpa*	11555	*Adrb2*
	11450	*Adipoq*	17777	*Mttp*	20296	*Ccl2*
	11806	*Apoa1*	19013	*Ppara*	15368	*Hmox1*
	66113	*Apoa5*	..	..	16193	*Il6*
	11832	*Aqp7*	..	..	16847	*Lepr*
	12606	*Cebpa*	..	..	19084	*Prkar1a*
	12683	*Cidea*	..	..	18787	*Serpine1*
	12944	*Crp*	..	..	..	..
	12974	*Cs*	..	..	..	..
	93747	*Echs1*	..	..	..	..
	58991	*Ghrl*	..	..	..	..
	15894	*Icam1*	..	..	..	..
	59027	*Nampt*	..	..	..	..
	103968	*Plin1*	..	..	..	..
	19016	*Pparg*	..	..	..	..
	19084	*Prkar1a*	..	..	..	..
	19088	*Prkar2b*	..	..	..	..
	18787	*Serpine1*	..	..	..	..
	20917	*Suclg2*	..	..	..	..
	22227	*Ucp1*	..	..	..	..
Historical version	In silico discovery with the GSE145840 series database. March 03, 2023					

The statistically significant pathways with GSEA enrichment in the FAT-$PM_{2.5}$-CEJUS signature were the peroxisome proliferator-activated receptors (PPAR) signaling pathway, with −1.536 normalized enrichment points, and the small molecule transport with −1.328 normalized points (Fig. 4). The PPAR pathway has the entry mmu03320 in KEGG. It is a cell pathway mediated by PPAR receptors, which bind to fatty acids and act as TF. The signature influences this pathway through PPAR gamma receptors, reducing the expression of *Apoa1, Apoa5*, and *Ucp1*, limiting lipid transport and adaptive thermogenesis (Fig. 5).

The small molecule transport, with the id R-MMU-382551 in Reactome, participates partially in transport mediated by ABC family proteins through the ApoA1/ABCA7-1 complex, essential for the extracellular transport of phospholipids and cholesterol. This

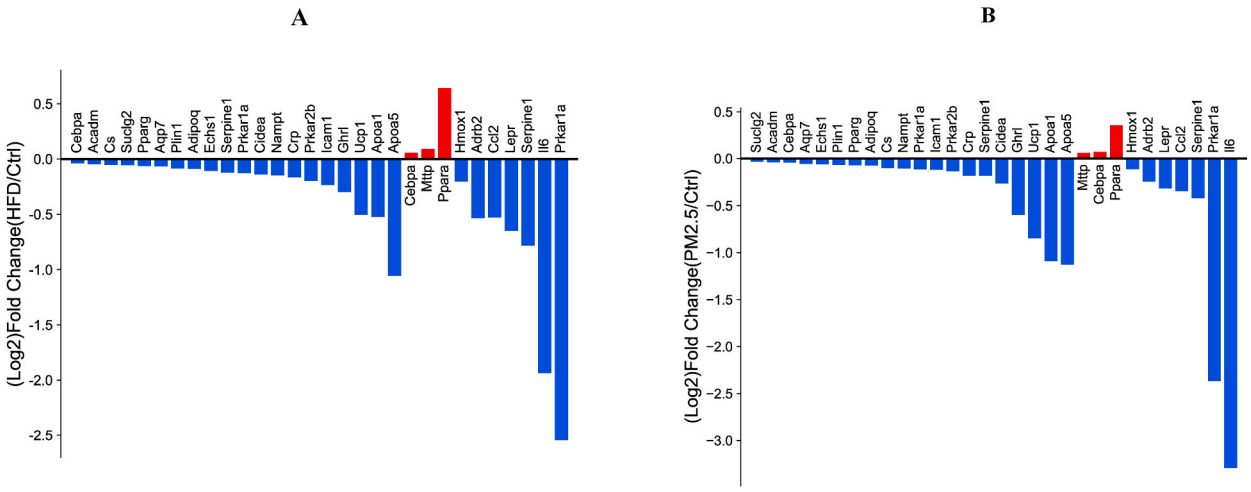

Fig. 3. Expression ratio induced by HFD and by $PM_{2.5}$ in the new transcriptomic signatures
A, the ratio of expression change for the three transcriptional signatures induced by high-fat diet (HFD). B, the ratio of expression change for the three transcriptional signatures induced by $PM_{2.5}$.
In A and B, the blue bars on the left correspond to the FAT-$PM_{2.5}$-CEJUS signature, the red bars to FAT- $PM_{2.5}$-UP, and the blue bars on the right to FAT- $PM_{2.5}$-DN signature.
Graphics designed in SRPlot (https://www.bioinformatics.com.cn/en). (For interpretation of the references to colour in this figure legend, the reader is referred to the Web version of this article.)

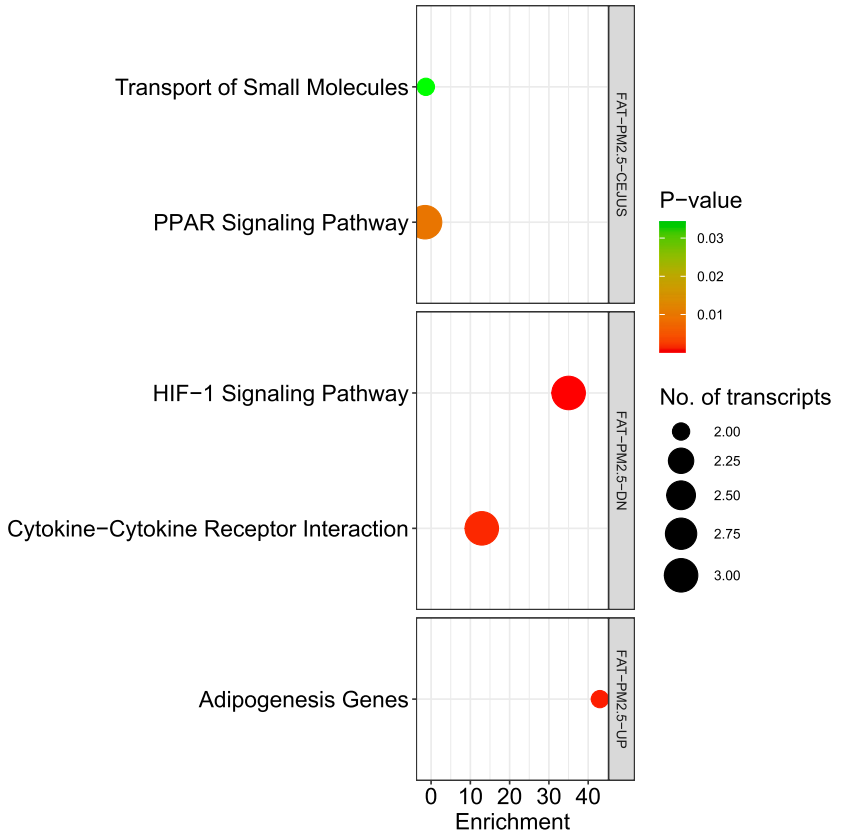

Fig. 4. Biological pathways significantly enriched in the FAT-$PM_{2.5}$-CEJUS, FAT- $PM_{2.5}$-UP, and FAT- $PM_{2.5}$-DN signatures
Graphic design in SRPlot (https://www.bioinformatics.com.cn/en).

signature also participates in lipid transport by converting chylomicrons (with apolipoproteins A and C coating) to residual chylomicrons through the action of lipoprotein lipase (LPL), co-activated by Apoa5 and Apoc, stimulating triglyceride (TG) hydrolysis to maintain lipid homeostasis and remodel plasma lipoproteins.

The adipogenesis gene pathway, with the WikiPathways entry WP447, was significant in the FAT-$PM_{2.5}$-UP signature with an ORA enrichment ratio of 42.984 (Fig. 4). This signature contributes to the upregulation of *Ppara* and *Cebpa*, which encode TFs related to adipogenic genes (Fig. 6).

The pathways with ORA enrichment in the FAT-$PM_{2.5}$-DN signature were the Hypoxia-Inducible Factor-1 (HIF-1) signaling pathway, with an enrichment ratio of 35.02, and the cytokine-cytokine receptor interaction, with an enrichment ratio of 12.909 (Fig. 4). The HIF-1 signaling pathway has the entry mmu04066 in KEGG, is activated in response to hypoxia, and is regulated by the HIF-1 transcription factor. In this pathway, genes like *Il-6, Hmox1*, and *Serpine1* participate, affecting the response to hypoxia in the context of exposure to a high fat diet and $PM_{2.5}$ (Fig. 7). The cytokine-cytokine receptor interaction pathway has the entry mmu04060 in KEGG and involves three genes: *Ccl2* (chemokine 2), *Il-6* (IL-6), and *Lepr* (leptin receptor), partially influencing cellular communication and the inflammatory response (Fig. 8).

3.2. Prediction of coordinated transcription regulatory elements

The FAT-$PM_{2.5}$-CEJUS signature showed a predominance of biased expression in 50% of its genes. In contrast, FAT-$PM_{2.5}$-UP presented three different types of expression for each of its three genes. At the same time, FAT-$PM_{2.5}$-DN was mainly characterized by

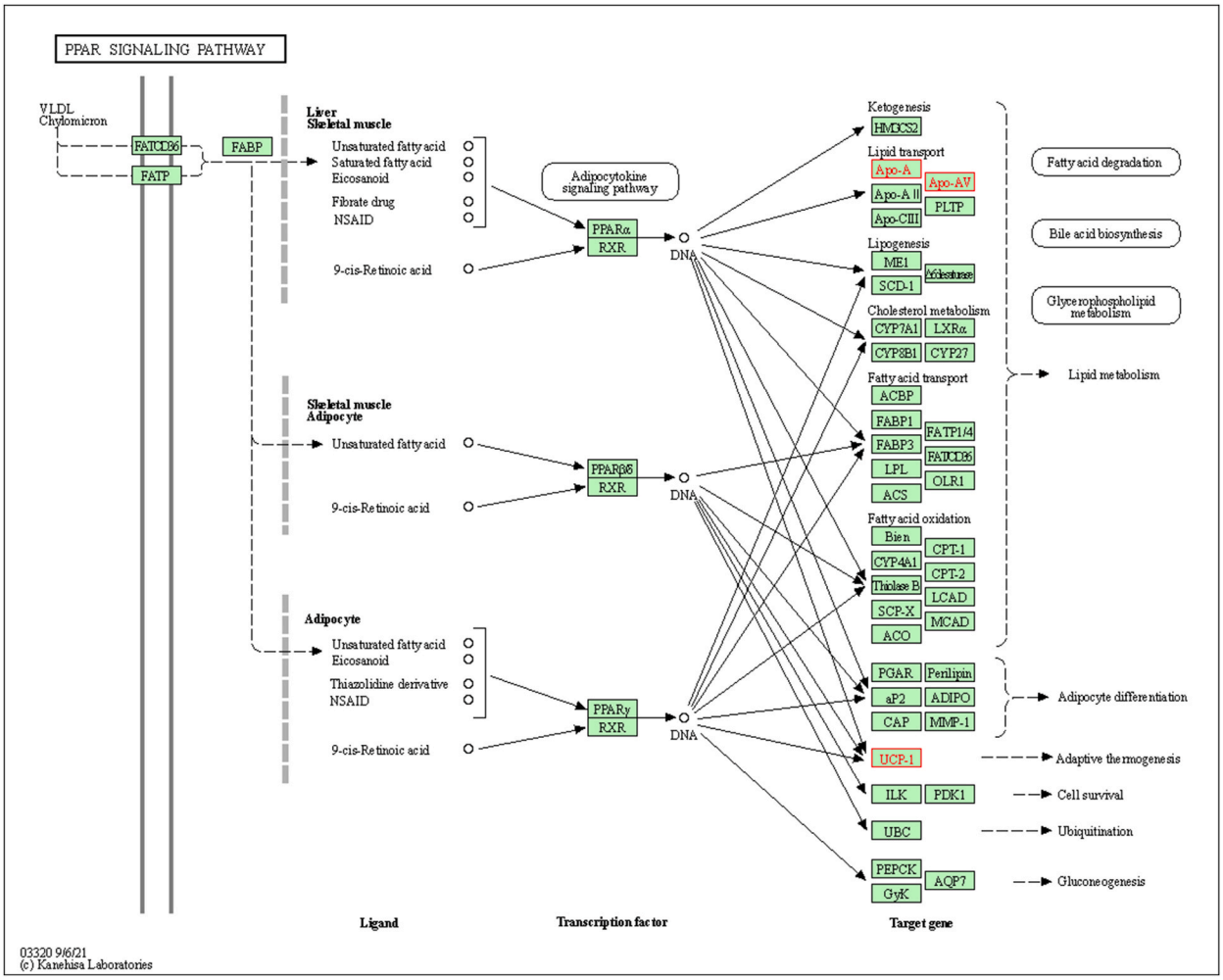

Fig. 5. KEGG network diagram of the PPAR signaling pathway
White boxes: biological pathway maps. Green boxes: genes or genetic products. Circles: molecules. Solid line arrows: direct relationship or molecular interaction. Dashed line arrows: indirect relationship or unknown reaction. Green boxes + arrows + circles + arrows = gene expression relationship. In red are the genes participating in the FAT-$PM_{2.5}$-CEJUS signature in this pathway. (For interpretation of the references to colour in this figure legend, the reader is referred to the Web version of this article.)

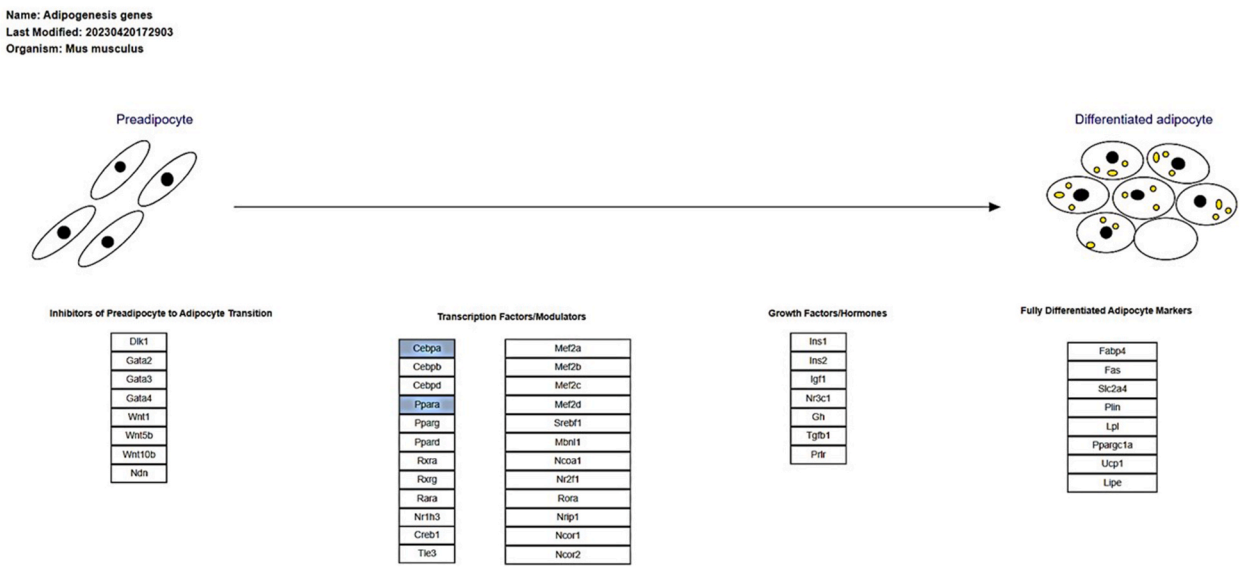

Fig. 6. WikiPathways diagram of adipogenesis genes
In blue, the genes participating in the FAT- $PM_{2.5}$-UP signature in the adipogenesis gene pathway. (For interpretation of the references to colour in this figure legend, the reader is referred to the Web version of this article.)

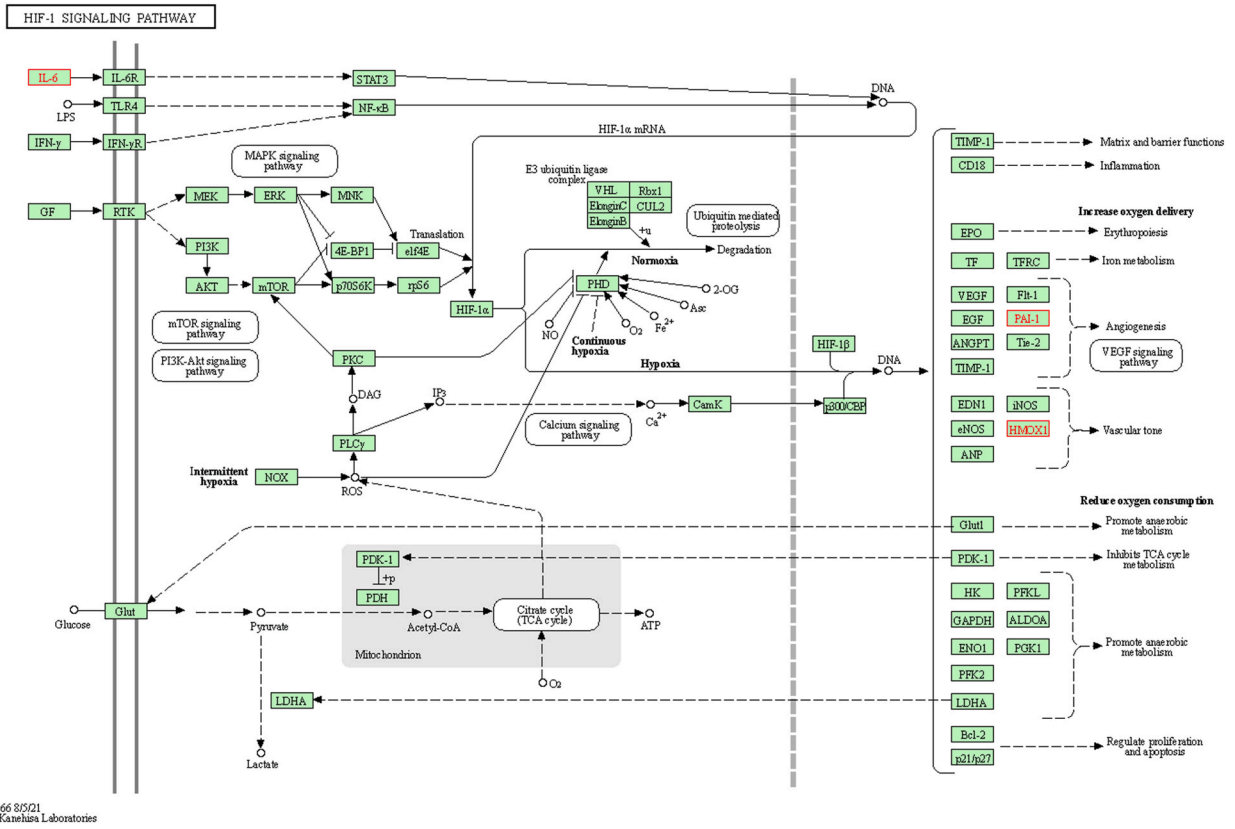

Fig. 7. KEGG network diagram of the HIF-1 signaling pathway
White boxes: biological pathway maps. Green boxes: genes or genetic products. Circles: molecules. Solid line arrows: direct relationship or molecular interaction. Dashed line arrows: indirect relationship or unknown reaction. Perpendicular lines: repression. +p: phosphorylation. +u: ubiquitination. Green boxes + arrows + circles + arrows = gene expression relationship. In red are the proteins encoded by the FAT-$PM_{2.5}$-DN signature in this pathway. (For interpretation of the references to colour in this figure legend, the reader is referred to the Web version of this article.)

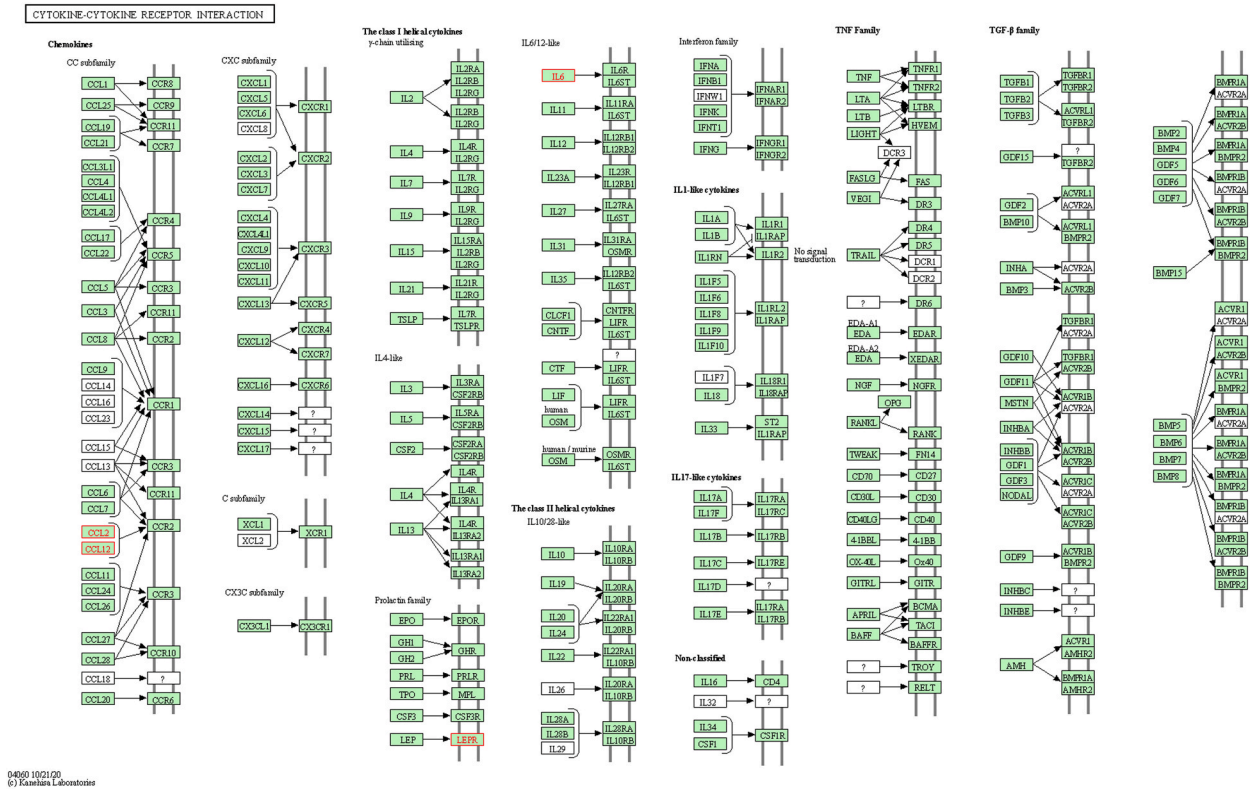

Fig. 8. KEGG network diagram of cytokine-cytokine receptor interaction
Large white box: biological pathway map. Small green boxes: genes or genetic products. Solid, black-tipped arrows: direct relationship or molecular interaction. In red are the proteins encoded by the FAT- $PM_{2.5}$-DN signature in this pathway. (For interpretation of the references to colour in this figure legend, the reader is referred to the Web version of this article.)

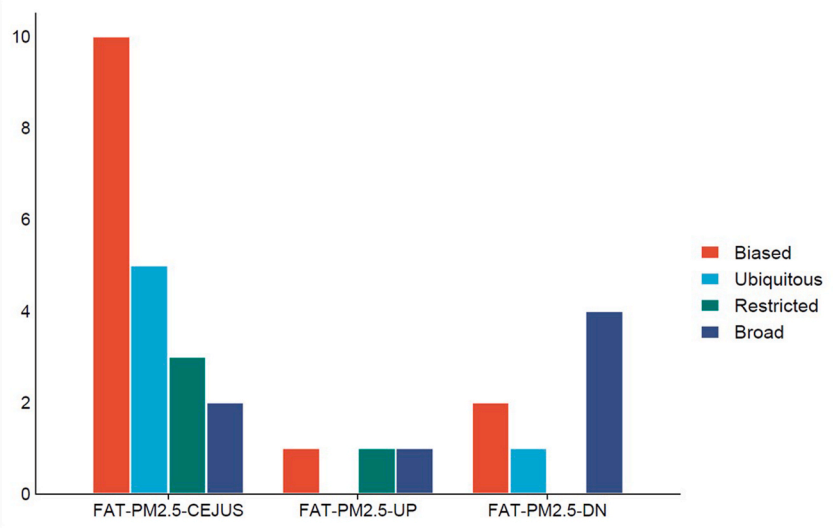

Fig. 9. The main types of expression for the FAT-$PM_{2.5}$-CEJUS, FAT-$PM_{2.5}$-UP, and FAT-$PM_{2.5}$-DN signatures are biased and broad
Graphic design in SRPlot (https://www.bioinformatics.com.cn/en).

broad expression, encompassing 57% of its genes (Fig. 9). In the latter, according to NCBI, common tissues of expression include liver tissue, mammary glandular tissue, in addition to adipose tissue.

Most of the genes composing each of the three new transcriptional signatures presented unique promoters, predominantly located on the coding strand of DNA. Regarding the analysis of regulatory elements in the core region of the promoters, only the initiator

Table 3
Promoter regions of the genes from the FAT-$PM_{2.5}$ -CEJUS, FAT-$PM_{2.5}$ -UP, and FAT-$PM_{2.5}$ -DN signatures.

Gene symbol	Promoter		
	ID	Core region	Position
		FAT-$PM_{2.5}$-CEJUS	
Acadm	Acadm_1	gggcgggaccccgtccgttttgcttgctgcacgga ggtggtcggaggcAGCAGATCGAG	Chromosome [NC_000069·6]; Strand [-]; Position [153944444]
Adipoq	Adipoq_1	ccccatgagtaccagactaatgagacctggccacttt ctcctcatttctGTCTGTACGAT	Chromosome [NC_000082·6]; Strand [+]; Position [23146604]
Apoa1	Apoa1_1	cccagccctgcccacacacatatatagaccaggga agaagagctggacACCCAGACTGT	Chromosome [NC_000075·6]; Strand [+]; Position [46228709]
Apoa5	Apoa5_1	actccctggcgcctagagtataaagtaagagtgtctg ctctctgtgcccAGAACCGAGCA	Chromosome [NC_000075·6]; Strand [+]; Position [46268608]
	Apoa5_2	tctagtccctggctttgcctctcctcctgatcaagccttc atctaccttCCTTCTCAGGG	Chromosome [NC_000075·6]; Strand [+]; Position [46269072]
Aqp7	Aqp7_1	ccattaactcagccatgagttgaagggcagatgggc aggaggcagacttGAATCTCCTTT	Chromosome [NC_000070·6]; Strand [-]; Position [41045437]
	Aqp7_2	cccagaggcaggctcaagtgaggactcggagaccg cagagctacagttcAGTTGCAGCTT	Chromosome [NC_000070·6]; Strand [-]; Position [41047962]
	Aqp7_3	actcagtctccatggtgctactggtaagaacagagat gctattttgggcAGTGTGTATGG	Chromosome [NC_000070·6]; Strand [-]; Position [41048112]
Cebpa	Cebpa_1	ggggcgatgcccgaccctctataaaagcggtccccg cgcgggcctggccATTCGCGACCC	Chromosome [NC_000073·6]; Strand [+]; Position [35119293]
Cidea	Cidea_1	agccctgggtcgggctttggagactccagcatgcag acagcctgttaggACACTCCGCTC	Chromosome [NC_000084·6]; Strand [+]; Position [67343479]
	Cidea_2	ggcgtggctgatagggcagtgatttaagagacgcgg ctttgggacaggaGGACCCGCACC	Chromosome [NC_000084·6]; Strand [+]; Position [67343791]
Crp	Crp_1	ccctccatctgctatagttataaatctgaggatgggct gggcccgaggcAAGCGTTCCAG	Chromosome [NC_000067·6]; Strand [+]; Position [172698056]
Cs	Cs_1	tgggctgggcgcctgtgccggtttgtctacccttcccc tcagccgcctcCTTTCAACCTT	Chromosome [NC_000076·6]; Strand [+]; Position [128337802]
Echs1	Echs1_1	tctggggcggagcgattctgcaggcggggcgattct gtgggcggaacacATCGTCTCTCC	Chromosome [NC_000073·6]; Strand [-]; Position [140116408]
Ghrl	Ghrl_1	aattctaaggcacataacatggagatgaagtaggcta ccagaagaccctCTCTCCCCCAG	Chromosome [NC_000072·6]; Strand [-]; Position [113719465]
Icam1	Icam1_1	ccccgtgagccagagactataaaagcgccgcccgc ctcagtctgcacccAGTGCTAGTGC	Chromosome [NC_000075·6]; Strand [+]; Position [21015985]
Nampt	Nampt_1	cgagcgagcggtgacttaagcaacggagcgcagc gaagcccatttttctCCTTGCTCGCA	Chromosome [NC_000078·6]; Strand [+]; Position [32820513]
	Nampt_2	ccccttgtccccgggatgggcggggcgcggagccg ccgggaaagccgccGGAGCGCGCTG	Chromosome [NC_000078·6]; Strand [+]; Position [32820357]
Plin1	Plin1_1	ccaagattccctggagtggctgcaagtgtttctgagg aggagaccttccACAGCTGGGCT	Chromosome [NC_000073·6]; Strand [-]; Position [79732781]
	Plin1_2	agggagggagcctgtgaaagacaagcctgcgggct tctgatagatctggGATTCTGCTTT	Chromosome [NC_000073·6]; Strand [-]; Position [79732170]
Pparg	Pparg_1	agtagcctgggctgcttttatataagggacgcgagga ggtcaagaagggGCCTGGACCTC	Chromosome [NC_000072·6]; Strand [+]; Position [115362353]
	Pparg_2	agtgtgacgacaaggtgaccgggctgaggggacg ggctgaggagaagtcACACTCTGACA	Chromosome [NC_000072·6]; Strand [+]; Position [115361269]
	Pparg_3	taagctcgatgaccataagccttttttcctttaaccaacc aatcttttgcAAGACATAGAC	Chromosome [NC_000072·6]; Strand [+]; Position [115422056]
Prkar1a	Prkar1a_1	tgacgtcagcagccgaacgctgattggccgcggtcg gctggtttccggtGGAGCCGTCGC	Chromosome [NC_000077·6]; Strand [+]; Position [109650949]
	Prkar1a_2	ggtaggagggtcgaagggagggagaaaagacaga ggcgtggagggaggcAGACGCAAGAG	Chromosome [NC_000077·6]; Strand [+]; Position [109650542]
	Prkar1a_3	tttttccttccttttcttcagaacacgaccgggcatgctca gtgctatccAGTTCCCTCTC	Chromosome [NC_000077·6]; Strand [+]; Position [109649392]
Prkar2b	Prkar2b_1	gggcgggggcggcgcagcggcggcgggagca ggagcgggaggagctggAGATGCTGCCA	Chromosome [NC_000078·6]; Strand [-]; Position [32061277]
Serpine1	Serpine1_1	ttccggctcacatctggtataaagggaggcagcagc cagggaacggagcACAGCTGGATC	Chromosome [NC_000071·6]; Strand [-]; Position [137072268]
Suclg2	Suclg2_1	ggcgggctccctcctccgccccctccctccccctcg ccgcctctcttcaGGTTCCTGGTT	Chromosome [NC_000072·6]; Strand [-]; Position [95718789]
Ucp1	Ucp1_1	ctcctccggcaaggggctatatagatctcccaggtca gggcgcagaagtGCCGGGCAATC	Chromosome [NC_000074·6]; Strand [+]; Position [83290352]

FAT-PM$_{2.5}$-UP			
Cebpa	*See the information presented in FAT-PM$_{2.5}$-CEJUS signature.*		
Mttp	Mttp_1	acctttcccctatagataaacactgttgtcgccggttctgaag agggtcACTTCCTTGCT	Chromosome [NC_000069·6]; Strand [-]; Position [138131367]
	Mttp_2	cggagaaagaggaggagcctgtaggggcggggtctgg gcctgggttttGCGGGAATGGT	Chromosome [NC_000069·6]; Strand [-]; Position [138143370]
Ppara	Ppara_1	gtgggggcgcggctggcacgggcgcgcgtaggcggtgc cgggccggggcCCCGGACGCTA	Chromosome [NC_000081·6]; Strand [+]; Position [85735526]
	Ppara_2	ctcttgttctgtgagtgcagatctcaccctgctgctggggcag tccacaTGTGACTCTCA	Chromosome [NC_000081·6]; Strand [+]; Position [85770343]
FAT-PM$_{2.5}$-DN			
Adrb2	Adrb2_1	acgtcactgggcaattcccctaaagtctggtgcacat aacgggcagggcGCACTGCAAGG	Chromosome [NC_000084·6]; Strand [-]; Position [62179978]
Ccl2	Ccl2_1	tccacccccctggcttacaataaaaggctgcctcaga gcagccagaagtGCAGAGAGCCA	Chromosome [NC_000077·6]; Strand [+]; Position [82035577]
Hmox1	Hmox1_1	accacgtgacccgcgtacttaaagggctggcgcgg gcagctgctcgctcACGGTCTCCAG	Chromosome [NC_000074·6]; Strand [+]; Position [75093622]
Il6	Il6_1	ttagagagttgactcctaataaatatgagactggggat gtctgtagctcATTCTGCTCTG	Chromosome [NC_000071·6]; Strand [+]; Position [30013143]
Lepr	Lepr_1	ccagccggagcactcctttaaaaggatttgcagcggt gaggaaaaaaccAGACCCGACCG	Chromosome [NC_000070·6]; Strand [+]; Position [101717906]
	Lepr_2	gccgcgcagtcacctgagtggccagtgccccgcag cgtcgcgcccgcgcACGAGTGGTCG	Chromosome [NC_000070·6]; Strand [+]; Position [101717430]
	Lepr_3	aacatggaagtttgaagacgtatttgtaatctttttttctttt tttttttCTATAGACTGC	Chromosome [NC_000070·6]; Strand [+]; Position [101727942]
Prkar1a	*See the information presented in FAT-PM$_{2.5}$-CEJUS signature*		
Serpine1	*See the information presented in FAT-PM$_{2.5}$-CEJUS signature*		

In red is the Initiator element (Inr).

element (Inr) was detected in Apoa1_1 in the case of FAT-PM$_{2.5}$-CEJUS and Il6_1 in FAT-PM$_{2.5}$-DN. The chromosomal distribution of the genes in the three signatures was heterogeneous, suggesting a transcriptional regulation in trans (Table 3).

The promoter ID consists of two parts separated by an underscore ('_'). Generally, the first part is the gene symbol/ID associated with the promoter; the second part is a number indicating the hierarchy of the promoter's usage for that gene. For genes with multiple promoters, "_1″ marks the promoter with the highest usage (primary promoter) and is followed by all others in decreasing order of usage. The core region is a short sequence segment corresponding to the −49 to +10 region of the promoter. Transcribed and non-transcribed nucleotides are represented by uppercase and lowercase characters, respectively. Genomic position: a eukaryotic promoter is defined as a DNA sequence around a transcription start site. The positional reference to the initiation site is, therefore, the central part of a promoter entry. Its assignment is based directly on experimental data. Strands are labeled as the sense strand (also known as the coding strand or positive strand) and the antisense strand (non-coding strand or negative strand). In strand notation, the symbol "+" is used for the sense strand, and the symbol "-" is used for the antisense strand.

The relative location of the five motifs in the primary promoters of the genes composing the three new transcriptional signatures was distributed on both positive and negative strands (Tables 4–6). Each primary promoter of these signatures exhibited a conserved main motif. In FAT-PM$_{2.5}$-CEJUS, one of the main motifs was Acadm_1a, with four TFBs and a width of 34 bases (Table 4); in FAT-PM$_{2.5}$-UP, it was Cebpa_1A with five TFBs and a width of 15 bases (Table 5); and in FAT-PM$_{2.5}$-DN, it was Adrb2_1A, with five TFBs and a width of 21 bases (Table 6).

According to the Multiple Expectation Maximization Motif Elicitation (MEME suite) (https://meme-suite.org/meme/tools/meme), predictions regarding the relative location and spatial distribution of the five motifs in the primary promoters of genes in this signature are distributed across positive and negative strands. However, a primary motif has been identified, the most conserved in each primary promoter of the signature. The identified motifs are as follows: Acadm_1A, with four transcription factor binding sites (TFB) and a width of 34 bases; Adipoq_1A, with 5 TFB and a width of 29 bases; Aqp7_1B, with 5 TFB and a width of 50 bases; Cebpa_1A, with 5 TFB and a width of 15 bases; Cidea_1A, with 5 TFB and a width of 35 bases; Crp_1A, with 5 TFB and a width of 29 bases; Cs_1A, with 4 TFB and a width of 21 bases; Echs1_1B, with 5 TFB and a width of 20 bases; Grhl_1A, with 5 TFB and a width of 11 bases; Icam1_1B, with 5 TFB and a width of 15 bases; Nampt_1A, with 5 TFB and a width of 41 bases; Plin1_1A, with 2 TFB and a width of 28 bases; Pparg_1A, with 4 TFB and a width of 48 bases; Prkar1a_1A, with 5 TFB and a width of 21 bases; Prkar2b_1A, with 5 TFB and a width of 41 bases; Serpine1_1A, with 5 TFB and a width of 19 bases; and finally, Suclg2_1A with 5 TFB and a width of 29 bases.

According to the Multiple Expectation Maximization Motif Elicitation (MEME suite) (https://meme-suite.org/meme/tools/meme), predictions regarding the relative location and spatial distribution of the five motifs in the primary promoters of genes in this signature are distributed across both positive and negative strands. However, a primary motif has been recognized, being the most conserved in each primary promoter of the signature: Cebpa_1A, with five transcription factor binding sites (TFB) and a width of 15 bases; Mttp_1B, with 5 TFB and a width of 38 bases; and Ppara_1A, with 5 TFB and a width of 45 bases.

According to the Multiple Expectation Maximization Motif Elicitation (MEME suite) (https://meme-suite.org/meme/tools/meme),

Table 4
Relative positions and motif consensus in primary promoters of the FAT-$PM_{2.5}$-CEJUS signature genes.

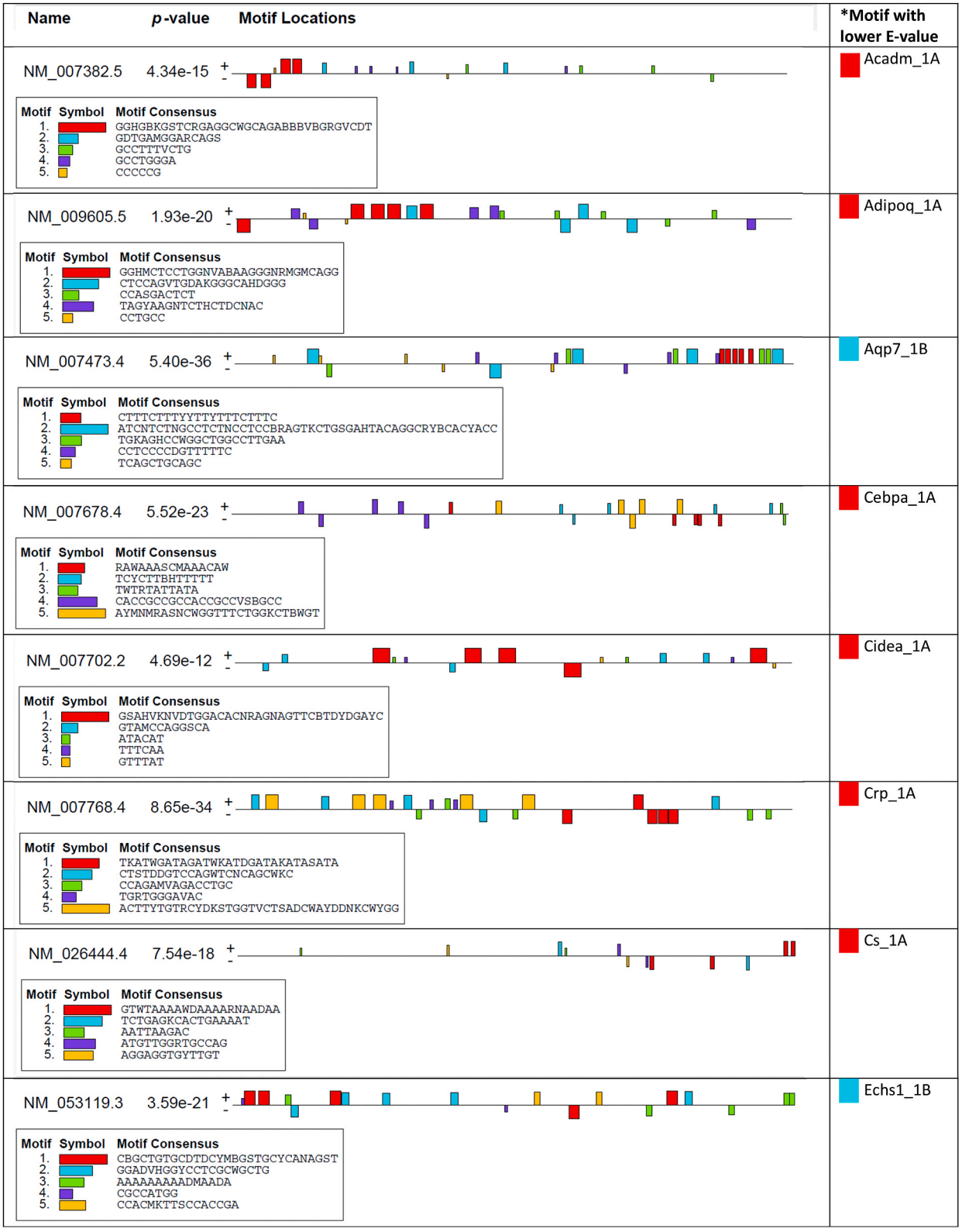

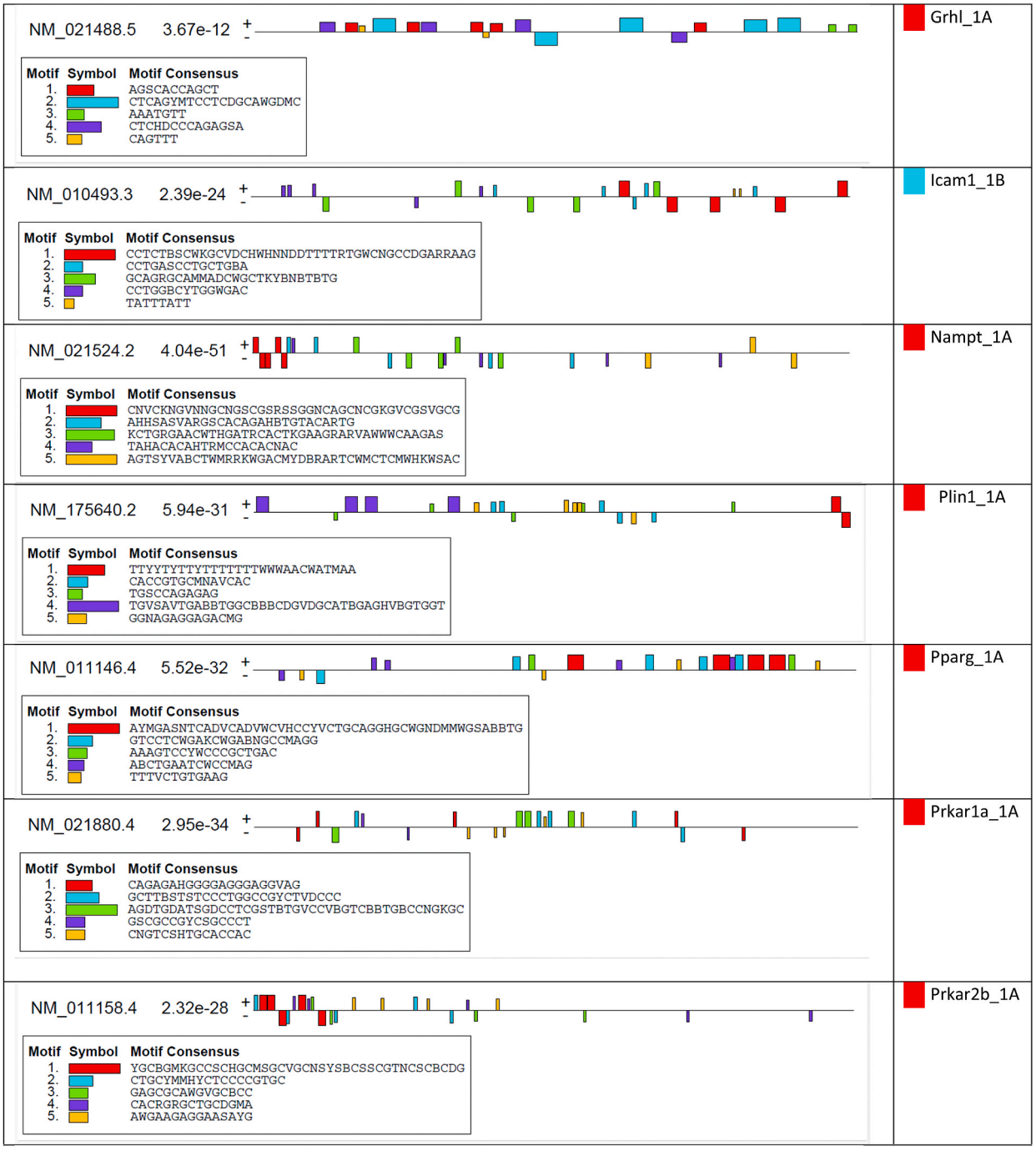
NM_021488.5 3.67e-12
Motif Symbol Motif Consensus
1. AGSCACCAGCT
2. CTCAGYMTCCTCDGCAWGDMC
3. AAATGTT
4. CTCHDCCCAGAGSA
5. CAGTTT
Grhl_1A
NM_010493.3 2.39e-24
Motif Symbol Motif Consensus
1. CCTCTBSCWKGCVDCHWHNNDDTTTTRTGWCNGCCDGARRAAG
2. CCTGASCCTGCTGBA
3. GCAGRGCAMMADCWGCTKYBNBTBTG
4. CCTGGBCYTGGWGAC
5. TATTTATT
Icam1_1B
NM_021524.2 4.04e-51
Motif Symbol Motif Consensus
1. CNVCKNGVNNGCNGSCGSRSSGGNCAGCNCGKGVCGSVGCG
2. AHHSASVARGSCACAGAHBTGTACARTG
3. KCTGRGAACWTHGATRCACTKGAAGRARVAWWWCAAGAS
4. TAHACACAHTRMCCACACNAC
5. AGTSYVABCTWMRRKWGACMYDBRARTCWMCTCMWHKWSAC
Nampt_1A
NM_175640.2 5.94e-31
Motif Symbol Motif Consensus
1. TTYYTYTTYTTTTTTTWWWAACWATMAA
2. CACCGTGCMNAVCAC
3. TGSCCAGAGAG
4. TGVSAVTGABBTGGCBBBCDGVDGCATBGAGHVBGTGGT
5. GGNAGAGGAGACMG
Plin1_1A
NM_011146.4 5.52e-32
Motif Symbol Motif Consensus
1. AYMGASNTCADVCADVWCVHCCYVCTGCAGGHGCWGNDMMWGSABBTG
2. GTCCTCWGAKCWGABNGCCMAGG
3. AAAGTCCYWCCCGCTGAC
4. ABCTGAATCWCCMAG
5. TTTVCTGTGAAG
Pparg_1A
NM_021880.4 2.95e-34
Motif Symbol Motif Consensus
1. CAGAGAHGGGGAGGGAGGVAG
2. GCTTBSTSTCCCTGGCCGYCTVDCCC
3. AGDTGDATSGDCCTCGSTBTGVCCVBGTCBBTGBCCNGKGC
4. GSCGCCGYCSGCCCT
5. CNGTCSHTGCACCAC
Prkar1a_1A
NM_011158.4 2.32e-28
Motif Symbol Motif Consensus
1. YGCBGMKGCCSCHGCMSGCVGCNSYSBCSSCGTNCSCBCDG
2. CTGCYMMHYCTCCCCGTGC
3. GAGCGCAWGVGCBCC
4. CACRGRGCTGCDGMA
5. AWGAAGAGGAASAYG
Prkar2b_1A

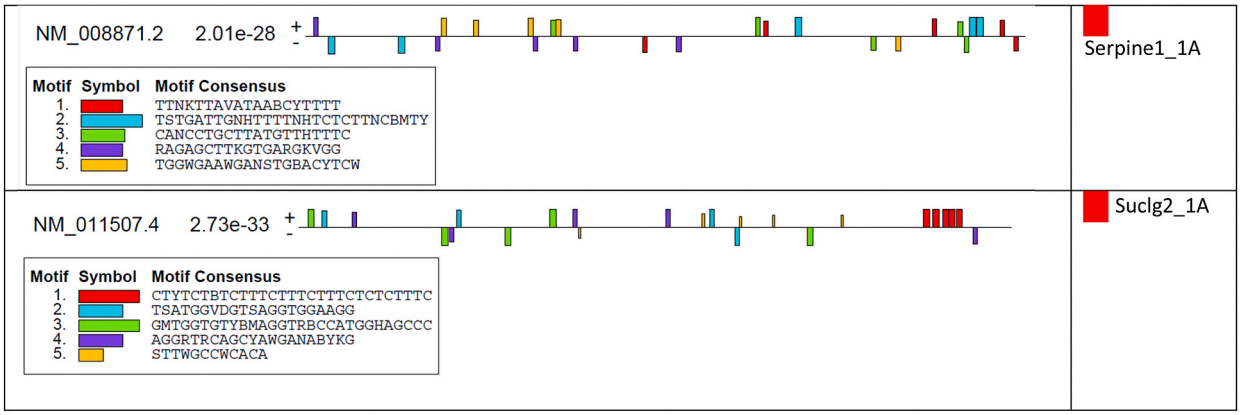

* In this research, the automatically assigned numbering of the motifs was replaced by their nomenclature, which consists of the first five letters of the alphabet.

Table 5
Relative positions and motif consensus in primary promoters of the FAT-$PM_{2.5}$-UP signature genes.

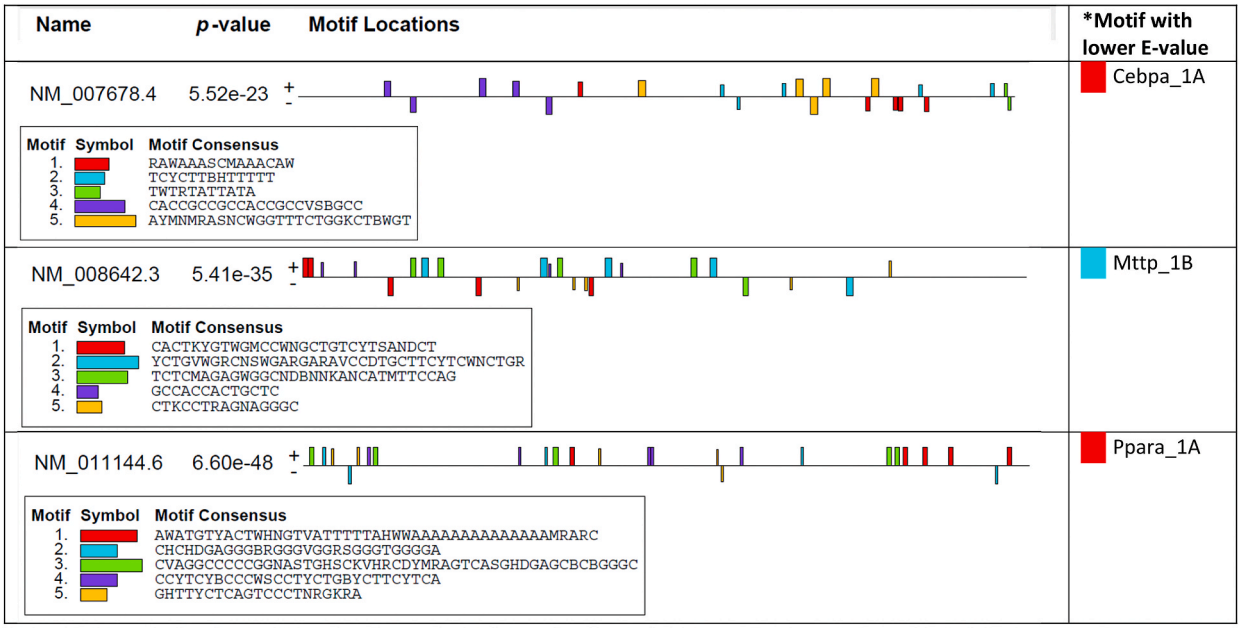

* In this research, the automatically assigned numbering of the motifs was replaced by their nomenclature, which consists of the first five letters of the alphabet.

predictions regarding the relative location and spatial distribution of the five motifs in the primary promoters of genes in this signature are distributed across positive and negative strands. The main motifs are Adrb2_1A, with five transcription factor binding sites (TFB) and a width of 21 bases; Ccl2_1A, with 5 TFB and a width of 13 bases; Il6_1A, with 5 TFB and a width of 15 bases; Lepr_1A, with 4 TFB and a width of 21 bases; and Prkar1a_1A, with 5 TFB and a width of 21 bases.

The other primary promoters of genes in the signatures showed specific characteristics regarding TFBs and width. In total, FAT-$PM_{2.5}$-CEJUS exhibited 125 TFBs in the main motif of its primary promoters, while FAT-$PM_{2.5}$-UP and FAT-$PM_{2.5}$-DN revealed the presence of 15 and 24 TFBs, respectively. Additionally, the sequences of the main motifs showed the four conserved nucleotide bases across the three signatures (see Table S10).

After the motif-motif similarity analysis of the TFBs in the three signatures, FAT-$PM_{2.5}$-CEJUS revealed 132 candidates TF for its

Table 6
Relative positions and motif consensus in primary promoters of the FAT-$PM_{2.5}$-DN signature genes.

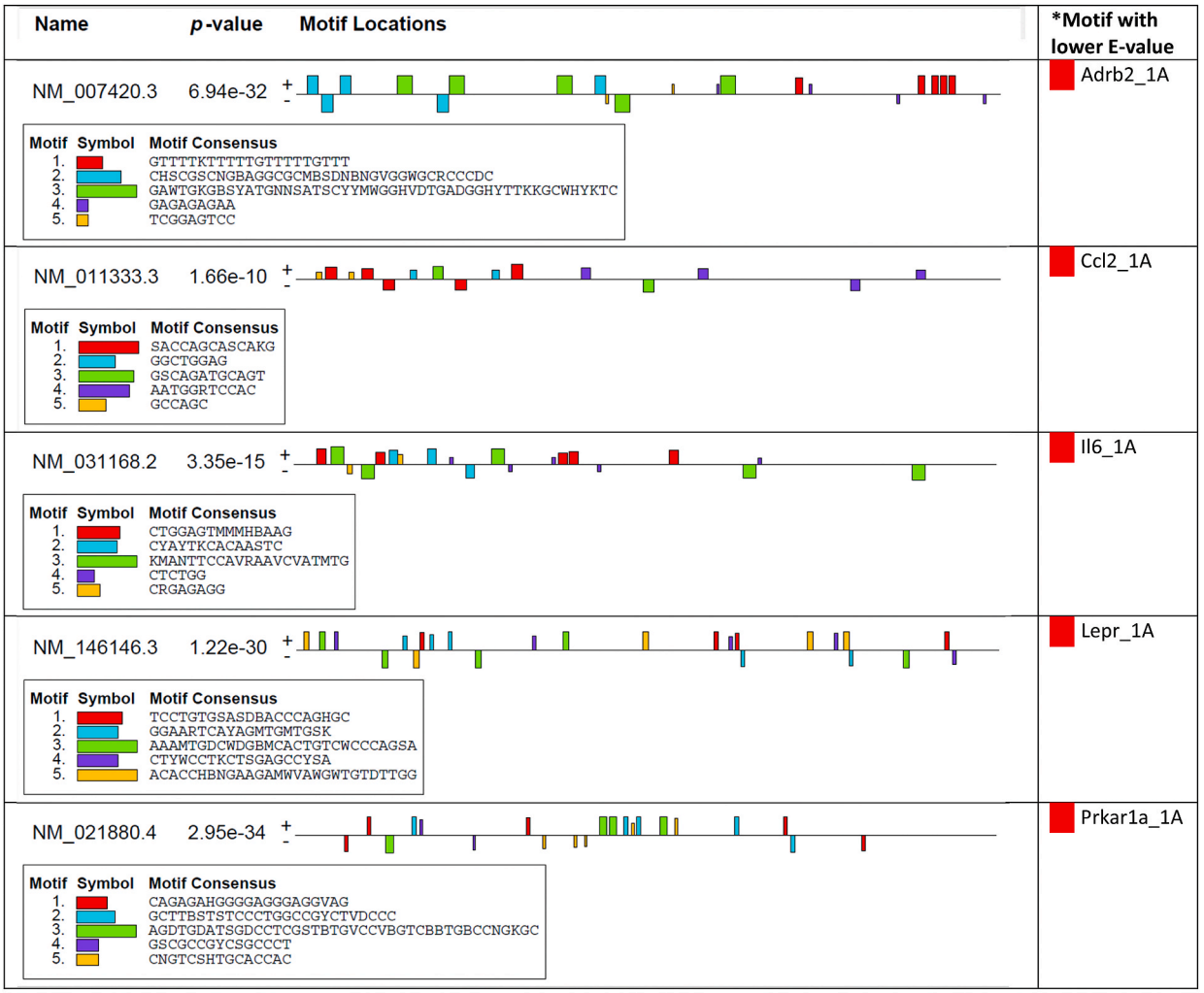

* In this research, the automatically assigned numbering to the motifs was replaced by their nomenclature, which consists of the first five letters of the alphabet.

125 TFBs; in FAT-$PM_{2.5}$-UP, 16 candidates TF for its 15 TFBs; and in FAT-$PM_{2.5}$-DN, 130 candidates TF for its main and alternative motifs. Common candidates TF were detected among the signatures, such as Zic1Zic2 in the primary promoters of *Icam1, Nampt, Acadm, Aqp7, Pparg,* and *Prkar1a* in FAT-$PM_{2.5}$-CEJUS. Additionally, *Pparg* and *Prkar2b* share TCF4. *Plin1, Cebpa*, and *Cidea* share ONECUT1 and Plagl1, with the latter also associated with *Adipoq*. In FAT-$PM_{2.5}$-UP, the primary promoters of *Ppara* and *Cebpa* share common TFs: Bcl11B, ONECUT1, and ONECUT3. *Mttp* has a common TF with *Ppara*, ZNF610. In FAT-$PM_{2.5}$-DN, TFIID could bind to the Inr in the core region of the *Il6* gene. The primary promoters of *Adrb2, Prkar1a, Ccl2*, and *Lepr* share common TFs: TCF4 and TFAP4ETV1 (the primary motifs of primary promoters and their associated transcription factors for signatures FAT-$PM_{2.5}$-CEJUS, FAT-$PM_{2.5}$-UP, and FAT-$PM_{2.5}$-DN are detailed in the see Table S10. These common TFs could facilitate coordinated regulation in each signature.

The presence of CGI was predicted in seven primary gene promoters in the FAT-$PM_{2.5}$-CEJUS signature, two in FAT-$PM_{2.5}$-UP, and two in FAT-$PM_{2.5}$-DN (see Fig. S5). In FAT-$PM_{2.5}$-CEJUS, the promoters Acadam_1, Cebpa_1, and Prkar2b_1 showed CGI covering both the promoter region and the gene body (appendix p 40). In FAT-$PM_{2.5}$-UP, Cebpa_1 exhibited a CGI spanning both regions (appendix p 41). FAT-$PM_{2.5}$-DN showed CGI in Adrb2_1 and two in Prkar1a_1 (appendix p 42) (Table 7). The results suggest a moderate presence of CGI in the promoters of these signatures.

Table 7
Putative CpG islands (CGI) in primary promoters of genes from the FAT-$PM_{2.5}$-CEJUS, FAT-$PM_{2.5}$-UP, and FAT-$PM_{2.5}$-DN signatures.

Primary Promoter ID	Putative CGIs			
	Number	Length	Position	UCSC Genome Browser on Mouse (GRCm39/mm39)
FAT-$PM_{2.5}$-CEJUS				
Acadam_1	1	505	57..561	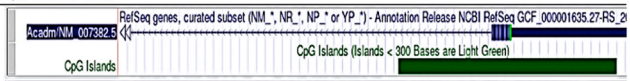
Cebpa_1	1	1445	47..1491	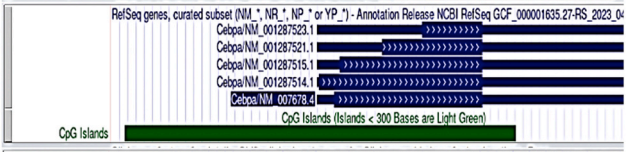
Cidea_1	1	207	49..255	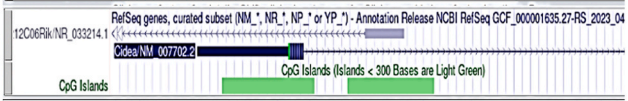
Nampt_1	1	245	47..291	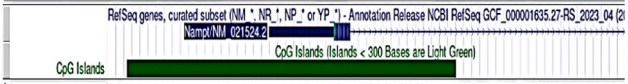
Plin1_1	1	448	1293..1740	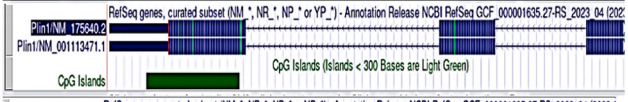
Prkar1a_1	2	258	501..758	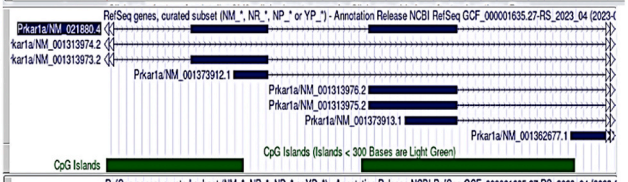
		209	1710..1918	
Prkar2b_1	1	520	47..566	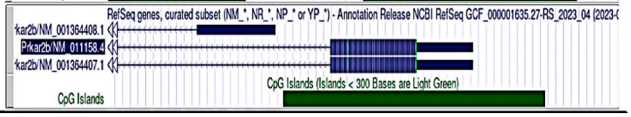
FAT-$PM_{2.5}$-UP				
Cebpa_1	1	1445	47..1491	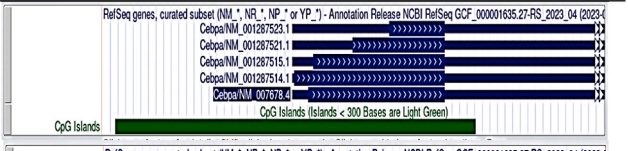
Ppara_1	2	248	686..933	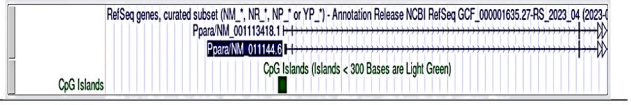
		207	1075..1281	
FAT-$PM_{2.5}$-DN				
Adrb2_1	1	422	51..472	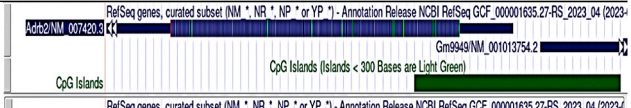
Prkar1a_1	2	258	501..758	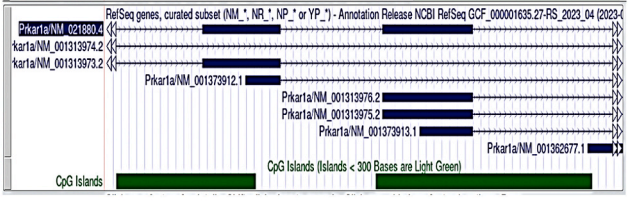
		209	1710..1918	

4. Discussion

The Rothman causality model allowed inferring at the beginning of this research that long-term exposure to $PM_{2.5}$ is not a sufficient cause to induce obesity but rather a contributing factor. Thus, these particles would interact with obesogenic factors, accelerating the development of metabolically abnormal obesity through the dysregulation of transcriptional signatures. Based on the obtained results, three new transcriptional signatures associated with metabolically abnormal obesity are proposed: FAT-$PM_{2.5}$-CEJUS, FAT-$PM_{2.5}$-UP, and FAT-$PM_{2.5}$-DN. The similarity of the transcriptional regulation profile in adipocytes, both due to HFD intake and chronic exposure to $PM_{2.5}$, indicates a potential mechanistic interaction between these factors.

However, the effect of HFD and $PM_{2.5}$ on the obese phenotype and abnormal metabolism was distinct. According to the reports by Rajagopalan et al. [33], it was identified that mice exposed to HFD developed moderately metabolically abnormal obesity, while mice exposed to ~60–120 μg/m^3 of $PM_{2.5}$ exhibited severe abnormal metabolism without obesity. In contrast, Si et al. [66] observed subcutaneous white adipose tissue hypertrophy in mice exposed to $PM_{2.5}$ for eight weeks while being fed a normal diet. This discrepancy could be explained based on the origin of the studied white adipose tissue. Rajagopalan et al. [33] analyzed adipocytes from epididymal adipose tissue, while Si et al. [66] studied subcutaneous adipose tissue.

In mice, epididymal adipose tissue is representative of visceral adipose tissue [67], and as known, this adipose tissue differs from subcutaneous adipose tissue [68]: i. Subcutaneous adipose tissue presents a heterogeneous mixture of mature unilocular adipocytes interspersed with small multilocular adipocytes of significantly reduced diameter, providing a higher density of adipocytes in this tissue compared to visceral adipose tissue [67]. ii. Subcutaneous adipose tissue contains a higher number of immune cells than visceral tissue [67], such as macrophages/monocytes, eosinophils, neutrophils, ILC2, T and B cells, dendritic cells, NK cells [69,70], in comparison to visceral adipose tissue [67]. iii. Kim et al. [71] reported that mice fed with HFD had a 98% and 166% increase in the size of epididymal and subcutaneous adipocytes, respectively, compared to mice fed a normal diet.

Therefore, the results obtained by Si et al. [66] may be attributed to the high dose of $PM_{2.5}$ to which the mice were exposed and the nature of the studied adipose tissue, which has a greater potential for hypertrophy, higher immunological response to foreign agents, and higher weight than visceral adipose tissue. Possibly, the subcutaneous adipose tissue, containing a higher number of immune cells, exhibited an innate response [72] to the elevated dose of $PM_{2.5}$ to which the mice were exposed, in comparison to the exposure dose of the rodents studied by Rajagopalan et al. [33]. According to the findings of Okada et al. [73], observed the intracellular behavior of these particles in live mammalian cells in culture media; these particles gradually form aggregates starting from 5 h of exposure. The high doses of $PM_{2.5}$ could have favored the formation of larger aggregates, which, in turn, may have induced mechanical damage to organelles, primarily mitochondria, affecting pathways involved in electron transport [74]. This, in turn, could promote the generation of reactive oxygen species (ROS), their accumulation, and oxidative stress.

Chen et al. [75] hypothesized the link between innate immune response and oxidative stress. They suggest that while the innate immune system lacks the fine specificity of adaptive immunity necessary for generating immunologic memory, it can distinguish between self and foreign molecules through pattern recognition receptors. These receptors detect a range of molecular patterns associated with exogenous pathogens and endogenous pathological molecular patterns, the latter of which includes ROS. Endogenous patterns could trigger sterile inflammation by binding to pattern recognition receptors, promoting the recruitment of more immune cells to the site of injury, and amplifying the inflammatory response. This, in turn, could disrupt insulin signaling pathways, favoring hypertrophy of subcutaneous adipose tissue [76] as a compensatory mechanism to improve insulin sensitivity [77].

Now, the results obtained in this research are consistent with evidence published in recent decades. On the one hand, Yen et al. [78] studied 21 subjects with obesity, and all of them experienced some degree of abnormal metabolism. In contrast, the following authors reported different frequencies of subjects with metabolically normal obesity [79–83]. While metabolically abnormal obesity is reported, there is substantial evidence regarding metabolically normal obesity.

Contrary to the previous reports, as of June 2023, based on searches conducted on the Web of Science, there is no evidence yet that refers to individuals who, when directly exposed to $PM_{2.5}$, maintained normal metabolism or developed obesity. In this regard, several authors reported biological models that, following exposure to these particles, developed abnormal metabolism and/or alteration of biological pathways involved in metabolism [84–89]; moreover, Du et al. [90] reported that the combined treatment of $PM_{2.5}$ and HFD had a synergistic effect on the onset and development of fatty liver disease. Furthermore, several other authors have reported murine models that, following direct and exclusive exposure to $PM_{2.5}$, did not develop obesity [91–95]. However, regarding indirect or short-term exposures to $PM_{2.5}$ and their effect on the development of obesity, the evidence has been minimal and inconsistent, and the authors suggest further similar research to assess result reproducibility [96–99].

Therefore, in terms of Rothman, it is concluded that HFD is a sufficient cause for developing obesity, and $PM_{2.5}$ is a component cause and functional for the severe abnormal metabolism associated with obesity. This thesis could be supported by the first law of thermodynamics. Living organisms require the consumption of energy for biological processes to take place. The energy derived from food is chemical and transforms into mechanical, thermal, and electrical energy to sustain these processes [100,101]. The balance between intake and caloric expenditure is known as energy balance [102,103], a concept coined from the first law of thermodynamics [104,105] with three types of balances: neutral when there is energy balance, negative when expenditure exceeds consumption, and positive when energy intake surpasses caloric expenditure [105,106]. Unused energy is stored in glycogen as an energy reserve in striated muscle and the liver and in triglycerides for storage in adipose tissue and other organs, based on the gradient.

While the HFD and $PM_{2.5}$ exhibit a mechanistic interaction by inducing similar transcriptional profiles in the signatures FAT-$PM_{2.5}$-CEJUS, FAT-$PM_{2.5}$-UP, and FAT-$PM_{2.5}$-DN, affecting the same biological pathways equally, $PM_{2.5}$ are not molecules that can transform or transfer chemical energy, as do the nutritional components of the HFD. Therefore, $PM_{2.5}$ needs to interact with an energy substrate to generate severe metabolically abnormal obesity. Exposure to obesogenic environments would encourage the consumption of HFD,

and air pollution by $PM_{2.5}$ would exacerbate the metabolic disturbances present in obesity. Both exposures occur concurrently in space and time, which could favor the mechanistic interaction of these factors.

The most relevant finding presented in this research is that one of the genes that form part of the FAT-$PM_{2.5}$-CEJUS signature is *Ucp1*, and until recently, it was thought that this gene had restricted expression to brown adipocytes [107,108]. *Ucp1* was identified in the PPAR signaling pathway, and based on the transcriptional level of the FAT-$PM_{2.5}$-CEJUS signature, its regulation is downregulated, mediated by the PpargRxra complex. Consequently, the synthesis of the protein-encoding Uncoupling Protein 1 (UCP1) would also decrease, thus restricting adaptive thermogenesis, which involves the generation of heat by the organism in response to external stimuli.

Since the early mammals relied on their ability to occupy colder niches, adaptive thermogenesis was crucial for their success during evolution [109–111]. Generally, adaptive thermogenesis is divided into shivering (tremor) and non-shivering forms [112,113]. The only form of non-shivering and facultative adaptive thermogenesis in mammals relies on UCP1 [113]. UCP1 is a channel found in the inner membrane of mitochondria in adipocytes, and when activated, it catalyzes the leakage of protons generated by the electron transport chain to produce heat [114,115], known as uncoupling of oxidative phosphorylation [116,117].

In 2009, several research networks confirmed that adults have deposits of brown adipose tissue in the supraclavicular and neck region that express UCP1 and can be induced in response to cold exposure. However, follow-up studies showed that it can also be expressed in white adipose tissue [118]. Currently, the ability of progenitor cells, as well as mature adipocytes, to differentiate into a model resembling the brown cell profile has been demonstrated, and when it occurs in white adipocytes, it is known as the browning of white adipose tissue [111,115,119].

It has been demonstrated that the PPAR signaling pathway plays a key role in activating the browning process as a strategy to counteract obesity [120,121]. Therefore, the uncoupling of oxidative phosphorylation that should occur in the mitochondria of white adipocytes through browning to dissipate excess energy in the form of heat before storing it in TG droplets may be disrupted by the downregulation of *Ucp1* transcription with exposure to HFD and $PM_{2.5}$.

It is inferred that the three new transcriptional signatures would be integrated into a systemic biological process as a result of the mechanistic interaction between exposure to HFD and $PM_{2.5}$, which would induce a *trans*-regulation transcriptionally (Fig. 10). The details of this process are described below.

4.1. 1st chronic and concomitant exposure to HFD and $PM_{2.5}$

The lipids ingested from the HFD are absorbed in the small intestine, converted into micelles, and enter circulation, where they combine with apoproteins to form lipoproteins. In systemic circulation, they are transported to peripheral tissues. In adipose tissue, fatty acids are actively taken up through transporters such as fatty acid transport protein (FATP) and fatty acid-binding protein (FABP). They are then esterified into TG, contributing to storage in lipid droplets [122,123]. In brown adipocytes, the conversion of stored TG into energy is promoted through sympathetic activation of UCP-1 [124].

The inhaled $PM_{2.5}$ from contaminated air enters the respiratory tract and reaches the alveoli, where two-thirds are eliminated, and one-third move to the distal alveolar region. Type I + II epithelial cells, competing with surface macrophages, capture particles through

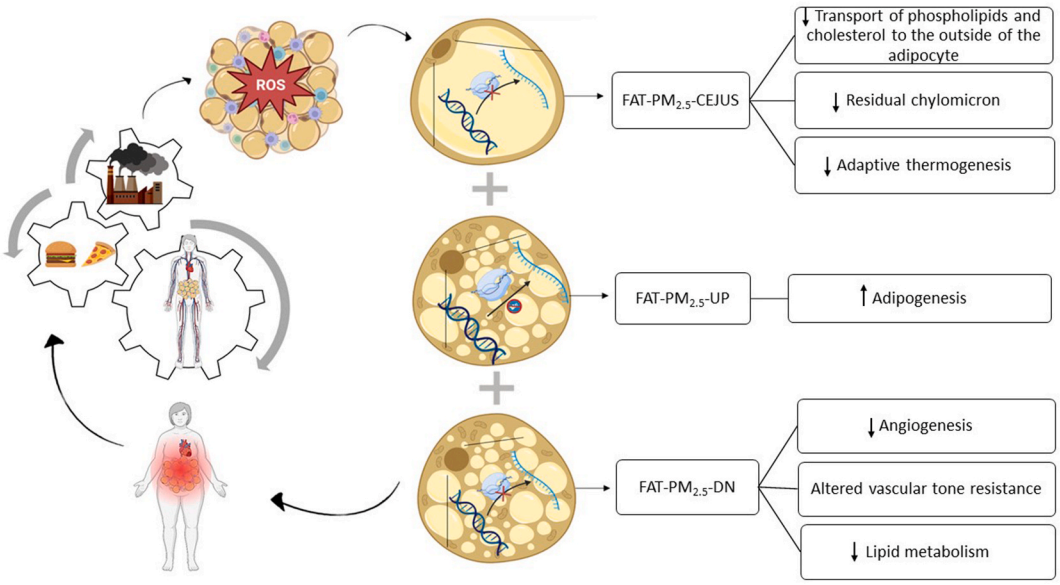

Fig. 10. Hypothesis of the underlying biological process for the mechanistic interaction of $PM_{2.5}$ with HFD in the etiology of severe metabolically abnormal obesity
Figure designed using the BioRender program (https://app.biorender.com/).

diffusion into the cytoplasm, enabling exocytosis. These particles then enter the systemic circulation, reaching adipocytes and entering through caveola-mediated endocytosis [99,125]. After 5 h, incorporated particles gradually aggregate, covered with structures resembling low-density intracellular white membranes, peaking at 9 h. By 24 h, aggregates decrease, suggesting these membranes may be autophagic structures [73]. The electric charge of $PM_{2.5}$ and the cytoplasm may favor electrostatic interactions facilitating aggregate formation.

4.2. 2nd initial cytotoxicity

As lipid overload progresses in the adipocyte, it initiates hypertrophic expansion, leading to mechanical and cellular stress [126,127]. Additionally, adaptive thermogenesis decreases in brown adipocytes [85,128].

As $PM_{2.5}$ aggregates, they may damage organelles, particularly the mitochondria. Mitochondria are known to generate significant amounts of hydrogen peroxide (H_2O_2) as a byproduct of cellular respiration and the respiratory chain process. Iron (Fe), the most abundant metal detected in the particles to which the experimental group of mice was exposed [129], would interact with H_2O_2 and, through the Fenton reaction, transform into the hydroxyl radical (OH•) by electron transfer: $Fe^{2+} + H_2O_2 \rightarrow Fe^{3+} + OH\bullet + OH\text{-}$ [130,131]. This increase in ROS would promote a cellular oxidative stress environment.

4.3. 3rd Subchronic cytotoxicity

The accumulation of intramitochondrial lipids contributes to the dysfunction of this organelle [132,133], which, in turn, would decrease the production and activity of superoxide dismutase (SOD). Consequently, the superoxide radical $O_2{\cdot}-$, a byproduct of the cellular respiration process and respiratory chain [129], would increase its concentration [134]. This rise in ROS would favor a cellular oxidative stress environment.

The continuous formation of $PM_{2.5}$ aggregates leads to a sustained presence and accumulation of ROS, with corresponding cellular repercussions.

4.4. 4th Chronic cytotoxicity

The oxidative stress can lead to oxidative modification of common TFs in the FAT-$PM_{2.5}$-CEJUS and FAT-$PM_{2.5}$-DN signatures, promoting the formation of covalent cross-links between amino acid residues. For example, when oxidation occurs on a cysteine present in the protein structure of the common TF, it can form a covalent bond with another oxidized cysteine, creating a cross-linked disulfide bridge (-S-S-) between the two cysteine residues. This process is known as the formation of cross-linked disulfide bonds [135]. Cross-links alter the three-dimensional structure, thus affecting the interaction of common TF candidates with the subsequent TFBs and their respective biological repercussions.

In FAT-$PM_{2.5}$-CEJUS: Pparg_1A, downregulating the transcription of the *Pparg* gene and, in turn, the synthesis of the PPARG receptor, thus affecting the formation of the PpargRxra complex; consequently, the transcription of the genes *Apoa 1, Apoa5*, and *Ucp1* would also be downregulated. Based on the chronicity of exposures to HFD and $PM_{2.5}$, a prevailing negative feedback loop effect would persist. This transcriptional regulation would decrease in the white adipocyte the transport of phospholipids and cholesterol outside the cell, the formation of residual chylomicrons, and adaptive thermogenesis. Icam1_1B, Nampt_1A, Acadm_1A, Aqp7_1B, Prkar1a_1A, Prkar2b_1A, Plin1_1A, Cebpa_1A, Cidea_1B, C, D, and E; Adipoq_1A, Serpine_1A, Crp_1A, Echs1_1B, Suclg2_1A, and Cs_1A; downregulating the transcription of the corresponding genes and the proteins they encode; thus, affecting the signaling and transport pathways that complement the previous ones.

In FAT-$PM_{2.5}$-DN: , the core promoter region of the *Il6* gene downregulates the transcription of the *Il6* gene and, consequently, the synthesis of the IL-6 cytokine, thus affecting the activation of the HIF-1 complex. Consequently, the transcription of the *Hmox1* and *Serpine1* genes would also be downregulated. Based on the chronicity of exposures to HFD and $PM_{2.5}$, a prevailing negative feedback loop effect would persist. This transcriptional regulation would decrease angiogenesis in brown adipocytes and affect vascular tone resistance. Ccl2_1B, C, D, and E; and Lepr_1B, C, D, and E; downregulating the transcription of the *Ccl2* and *Lepr* genes and, in turn, the synthesis of the C–C motif chemokine two and the leptin receptor in brown adipocytes. This promotes chronic low-intensity inflammation and decreases lipid metabolism. Adrb2_B, C, D, and E; and Prkar1a_B, C, D, and E; downregulating the transcription of the Adrb2 and Prkar1a genes and, consequently, the synthesis of beta-2 adrenergic receptor and protein kinase A regulatory subunit alpha. This affects the signaling pathways involved in plasma membrane rafts.

Oxidative stress can also impact DNA methyltransferase enzymes by oxidizing cysteine residues in their structure [136]. Cysteines contain a thiol group (-SH) in their side chain, which is susceptible to oxidation during oxidative stress. Oxidation of cysteines can lead to various forms of oxidative modification, including the formation of sulfenic cysteine (-SOH), disulfide cysteine (-S-S-), glutathione cysteine (-SSG), among others. These modifications can affect the catalytic activity and three-dimensional structure of enzymes [137], promoting hypomethylation of CGIs present in the promoters of the FAT-$PM_{2.5}$-UP signature. This could lead to the upregulation of transcription of the *Ppara* and *Cebpa* genes in brown adipocytes, consequently increasing the synthesis of the PPARA receptor and CCAAT/enhancer-binding protein alpha, promoting the transcription of related lipogenic genes. It is concluded that this biological process could operate as a negative feedback loop as long as the interaction between HFD and $PM_{2.5}$ persists.

About the main strengths of our research, we highlight the explanatory approach we adopted to analyze the causal relationship between chronic exposure to $PM_{2.5}$ and metabolically abnormal obesity using the Rothman causal model. This approach resulted in an innovative methodology, particularly in bioinformatics contexts, and to the best of our knowledge, it is the first study to employ it in

this manner. Another significant strength lies in the methodological rigor of our research design. In recent years, there has been an increase in the number of available molecular signatures; however, many of them exhibit redundancies both in composition and function and seldom show significance in statistical tests [138]. In this regard, the transcriptional signatures FAT- $PM_{2.5}$-CEJUS, FAT- $PM_{2.5}$-UP, and FAT- $PM_{2.5}$-DN are the outcome of a rigorous methodological and statistical process, allowing us to generalize in bioinformatics contexts and predict similar and reliable outcomes when experimentally validated.

In contrast, the main limitation of the study was that we were unable to conduct experimental in vitro research. In countries and entities with medium to low economies, there are difficulties in developing skills and accessing laboratories with the necessary technology for knowledge advancement [139,140]. Therefore, the availability of raw molecular data in open-access repositories [141, 142] presents an opportunity to overcome financial limitations that could hinder the testing of original hypotheses in omics sciences related to public health and environmental health. Another limitation was that we did not find a transcriptomic database in mice of the studied species where the same study group had been exposed to both $PM_{2.5}$ and HFD. In these cases, the TPM values of the transcriptional deregulation of the proposed signatures in this research may not correspond to the values reported here.

Our findings can have a significant impact on the formulation of public policies related to environmental health and obesity prevention. By demonstrating the link between chronic exposure to $PM_{2.5}$ and the development of severe metabolic alterations associated with obesity, we underscore the importance of addressing air quality as a key factor in public health. By adopting a comprehensive and multidisciplinary approach, we can implement effective measures to protect the population's health and enhance the quality of life in affected communities. Consequently, policymakers need to consider these findings when designing strategies to address the challenges of environmental health and the obesity pandemic.

Ethics declarations

Review and/or approval by an ethics committee was not needed for this study because it was a bioinformatics study based on annotations from public databases. Informed consent was not required for this study because our research did not involve the participation of human subjects.

Data availability statement

The data that support the findings of this study are openly available on the Open Science Framework (https://osf.io/t2657/).

CRediT authorship contribution statement

Sagrario Lobato: Writing – review & editing, Writing – original draft, Visualization, Validation, Software, Resources, Project administration, Methodology, Investigation, Funding acquisition, Formal analysis, Data curation, Conceptualization. **A. Lourdes Castillo-Granada:** Visualization, Validation, Supervision, Formal analysis. **Marcos Bucio-Pacheco:** Visualization, Supervision, Methodology, Conceptualization. **Víctor Manuel Salomón-Soto:** Writing – review & editing, Visualization, Supervision, Project administration, Formal analysis. **Ramiro Álvarez-Valenzuela:** Supervision, Project administration, Conceptualization. **Perla Margarita Meza-Inostroza:** Writing – review & editing, Validation, Supervision, Formal analysis. **Raúl Villegas-Vizcaíno:** Visualization, Validation, Supervision, Methodology, Formal analysis, Conceptualization.

Declaration of generative AI and AI-assisted technologies in the writing process

During the preparation of this work, the author(s) used Grammarly Premium to improve language and readability. After using this tool/service, the author(s) reviewed and edited the content as needed and take(s) full responsibility for the content of the publication.

Declaration of competing interest

The authors declare that they have no known competing financial interests or personal relationships that could have appeared to influence the work reported in this paper.

Acknowledgment

We extend our gratitude to DrPH Kenneth J. Rothman for his contributions to Epidemiology.

Appendix A. Supplementary data

Supplementary data to this article can be found online at https://doi.org/10.1016/j.heliyon.2024.e28936.

References

[1] M. Bluher, Obesity: global epidemiology and pathogenesis, Nat. Rev. Endocrinol. 15 (5) (2019) 288–298, https://doi.org/10.1038/s41574-019-0176-8.
[2] W.A.S. Aldamarany, H. Taocui, L.L. Deng, H. Mei, Z. Yi, G. Zhong, Perilla, sunflower, and tea seed oils as potential dietary supplements with anti-obesity effects by modulating the gut microbiota composition in mice fed a high-fat diet, Eur. J. Nutr. 62 (6) (2023) 2509–2525, https://doi.org/10.1007/s00394-023-03155-3.
[3] X. Lin, H. Li, Obesity: epidemiology, pathophysiology, and therapeutics, Front. Endocrinol. 12 (2021) 706978, https://doi.org/10.3389/fendo.2021.706978.
[4] U.J. Jung, Sarcopenic obesity: involvement of oxidative stress and beneficial role of antioxidant flavonoids, Antioxidants 12 (5) (2023) 25, https://doi.org/10.3390/antiox12051063.
[5] X. Wen, B.H. Zhang, B.Y. Wu, H.T. Xiao, Z.H. Li, R.Y. Li, et al., Signaling pathways in obesity: mechanisms and therapeutic interventions, Signal Transduct. Targeted Ther. 7 (1) (2022) 31, https://doi.org/10.1038/s41392-022-01149-x.
[6] A.A. Ahmed, H.H. Musa, M.E.A. Essa, A. Mollica, G. Zengin, H. Ahmad, et al., Inhibition of obesity through alterations of C/EBP- alpha gene expression by gum Arabic in mice with a high-fat feed diet, Carbohydr Polym Technol Appl 4 (2022) 10, https://doi.org/10.1016/j.carpta.2022.100231.
[7] T.N. Poly, M.M. Islam, H.C. Yang, M.C. Lin, W.S. Jian, M.H. Hsu, et al., Obesity and mortality among patients diagnosed with COVID-19: a systematic review and meta-analysis, Front. Med. 8 (2021) 11, https://doi.org/10.7326/M20-3742.
[8] J.M.V. Pino, V.F. Silva, M. Monico-Neto, D.C. Seva, M.Y. Kato, J.N. Alves, et al., Severe obesity in women can lead to worse memory function and iron dyshomeostasis compared to lower grade obesity, Internet J. Endocrinol. 2023 (2023) 7625720, https://doi.org/10.1155/2023/7625720.
[9] S.J. Huang, Y.H. Ma, Y.L. Bi, X.N. Shen, X.H. Hou, X.P. Cao, et al., Metabolically healthy obesity and lipids may be protective factors for pathological changes of alzheimer's disease in cognitively normal adults, J. Neurochem. 157 (3) (2021) 834–845, https://doi.org/10.1111/jnc.15306.
[10] J.M. Siurana, P.S. Ventura, D. Yeste, L. Riaza-Martin, L. Arciniegas, M. Clemente, et al., Myocardial geometry and dysfunction in morbidly obese adolescents (BMI 35-40 kg/m2), Am. J. Cardiol. 157 (2021) 128–134, https://doi.org/10.1016/j.amjcard.2021.07.026.
[11] L.P. Mayoral, G.M. Andrade, E.P. Mayoral, T.H. Huerta, S.P. Canseco, F.J. Rodal Canales, et al., Obesity subtypes, related biomarkers & heterogeneity, Indian J. Med. Res. 151 (1) (2020) 11–21, https://doi.org/10.4103/ijmr.IJMR_1768_17.
[12] W.J. Khalil, M. Akeblersane, A.S. Khan, A.S.M. Moin, A.E. Butler, Environmental pollution and the risk of developing metabolic disorders: obesity and diabetes, Int. J. Mol. Sci. 24 (10) (2023) 8870, https://doi.org/10.3390/ijms24108870.
[13] B. Bowe, A.K. Gibson, Y. Xie, Y. Yan, A. van Donkelaar, R.V. Martin, et al., Ambient fine particulate matter air pollution and risk of weight gain and obesity in United States veterans: an observational cohort study, Environ. Health Perspect. 129 (4) (2021) 10, https://doi.org/10.1289/EHP7944.
[14] I. Manisalidis, E. Stavropoulou, A. Stavropoulos, E. Bezirtzoglou, Environmental and health impacts of air pollution: a review, Front. Public Health 8 (2020) 14, https://doi.org/10.3389/fpubh.2020.00014.
[15] M. Amann, G. Kiesewetter, W. Schöpp, et al., Reducing global air pollution: the scope for further policy interventions, Philos Trans A Math Phys Eng Sci 378 (2183) (2020) 20190331, https://doi.org/10.1098/rsta.2019.0331.
[16] World Health Organization, WHO Global Air Quality Guidelines: Particulate Matter (PM2.5 and PM10), Ozone, Nitrogen Dioxide, Sulfur Dioxide and Carbon Monoxide, first ed., World Health Organization, Geneva, Swiss, 2021, pp. 12–92.
[17] Q. Zhou, M.M. Nizamani, H.Y. Zhang, H.L. Zhang, The air we breathe: an In-depth analysis of PM2.5 pollution in 1312 cities from 2000 to 2020, Environ. Sci. Pollut. Res. Int. 30 (41) (2023) 93900–93915, https://doi.org/10.1007/s11356-023-29043-1.
[18] S.J. Pai, T.S. Carter, C.L. Heald, J.H. Kroll, Updated World health organization air quality guidelines highlight the importance of non-anthropogenic PM (2.5), Environ. Sci. Technol. Lett. 9 (6) (2022) 501–506, https://doi.org/10.1021/acs.estlett.2c00203.
[19] J. Zhang, H. Cheng, A. Di Narzo, Y. Zhu, M. Shan, Z. Zhang, X. Shao, J. Chen, C. Wang, K. Hao, Within- and cross-tissue gene regulations were disrupted by PM2.5 nitrate exposure and associated with respiratory functions, Sci. Total Environ. 850 (2022) 157977, https://doi.org/10.1016/j.scitotenv.2022.157977.
[20] S. Zhang, J. Zhang, D. Guo, C. Peng, M. Tian, D. Pei, Q. Wang, F. Yang, J. Cao, Y. Chen, Biotoxic effects and gene expression regulation of urban PM2.5 in southwestern China, Sci. Total Environ. 753 (2021) 141774, https://doi.org/10.1016/j.scitotenv.2020.141774.
[21] C.M. Campolim, L. Weissmann, C.K.O. Ferreira, et al., Short-term exposure to air pollution (PM2.5) induces hypothalamic inflammation, and long-term leads to leptin resistance and obesity via Tlr4/Ikbke in mice, Sci. Rep. 10 (1) (2020) 10160, https://doi.org/10.1038/s41598-020-67040-3.
[22] M. Di Domenico, F. Pinto, L. Quagliuolo, et al., The role of oxidative stress and hormones in controlling obesity [published correction appears in front endocrinol (Lausanne). 2019 sep 27;10:693], Front. Endocrinol. 10 (2019) 540. https://doi:10.3389/fendo.2019.00540.
[23] R. Colebunders, A.K. Njamnshi, S. Menon, et al., Onchocerca volvulus and epilepsy: a comprehensive review using the Bradford Hill criteria for causation, PLoS Neglected Trop. Dis. 15 (1) (2021) e0008965. https://doi:10.1371/journal.pntd.0008965.
[24] M. Schoultz, M. Beattie, T. Gorely, J. Leung, Assessment of causal link between psychological factors and symptom exacerbation in inflammatory bowel disease: a systematic review utilising Bradford Hill criteria and meta-analysis of prospective cohort studies, Syst. Rev. 9 (1) (2020) 169. https://doi:10.1186/s13643-020-01426-2.
[25] M. Shimonovich, A. Pearce, H. Thomson, K. Keyes, S.V. Katikireddi, Assessing causality in epidemiology: revisiting Bradford Hill to incorporate developments in causal thinking, Eur. J. Epidemiol. 36 (9) (2021) 873–887. https://doi:10.1007/s10654-020-00703-7.
[26] M. Usman, Y. Hameed, M. Ahmad, Does human papillomavirus cause human colorectal cancer? Applying Bradford Hill criteria postulates, Ecancermedicalscience 14 (2020) 1107, https://doi.org/10.3332/ecancer.2020.1107.
[27] K.J. Rothman, Causes, Am. J. Epidemiol. 104 (6) (1976) 587–592.
[28] P. Boffetta, Causation in the presence of weak associations, Crit. Rev. Food Sci. Nutr. 50 (s1) (2010) 13–16. https://doi:10.1080/10408398.2010.526842.
[29] T.L. Lash, VanderWeele Tj, S. Haneuse, K.J. Rothman, Modern Epidemiology, 4th. ed, Wolters Kluwer, Mexico, 2021, pp. 97–1406.
[30] A.P. Davis, C.J. Grondin, R.J. Johnson, D. Sciaky, J. Wiegers, T.C. Wiegers, et al., Comparative Toxicogenomics database (CTD): update 2021, Nucleic Acids Res. 49 (D1) (2021) D1138–D1143.
[31] Y.X. Liao, J. Wang, E.J. Jaehnig, Z.A. Shi, B. Zhang, WebGestalt 2019: gene set analysis toolkit with revamped UIs and APIs, Nucleic Acids Res. 47 (W1) (2019) W199–W205, https://doi.org/10.1093/nar/gkz401.
[32] B.G. Patra, V. Maroufy, B. Soltanalizadeh, N. Deng, W.J. Zheng, K. Roberts, et al., A content-based literature recommendation system for datasets to improve data reusability - a case study on Gene Expression Omnibus (GEO) datasets, J. Biomed. Inf. 104 (2020) 8, https://doi.org/10.1016/j.jbi.2020.103399.
[33] S. Rajagopalan, B. Park, R. Palanivel, et al., Metabolic effects of air pollution exposure and reversibility, J. Clin. Invest. 130 (11) (2020) 6034–6040, https://doi.org/10.1172/JCI137315.
[34] W. Chen, J. Li, S.L. Huang, X.D. Li, X. Zhang, X. Hu, et al., GCEN: an easy-to-use toolkit for gene Co-expression network analysis and lncRNAs annotation, Curr. Issues Mol. Biol. 44 (4) (2022) 1479–1487, https://doi.org/10.3390/cimb44040100.
[35] A. Stupnikov, C.E. McInerney, K.I. Savage, S.A. McIntosh, F. Emmert-Streib, R. Kennedy, et al., Robustness of differential gene expression analysis of RNA-seq, Comput. Struct. Biotechnol. J. 19 (2021) 3470–3481, https://doi.org/10.1016/j.csbj.2021.05.040.
[36] Y.D. Zhao, M.C. Li, M.M. Konaté, L. Chen, B. Das, C. Karlovich, et al., TPM, fpkm, or normalized counts? A comparative study of quantification measures for the analysis of RNA-seq data from the NCI patient-derived models repository, J. Transl. Med. 19 (1) (2021) 15, https://doi.org/10.1186/s12967-021-02936-w.
[37] D.D. Bhuva, J. Cursons, G.K. Smyth, M.J. Davis, Differential co-expression-based detection of conditional relationships in transcriptional data: comparative analysis and application to breast cancer, Genome Biol. 20 (1) (2019) 21, https://doi.org/10.1186/s13059-019-1851-8.
[38] L.K. Brackmann, A. Poplawski, C.L. Grandt, H. Schwarz, T. Hankeln, S. Rapp, et al., Comparison of time and dose dependent gene expression and affected pathways in primary human fibroblasts after exposure to ionizing radiation, Mol. Med. 26 (1) (2020) 13, https://doi.org/10.1186/s10020-020-00203-0.
[39] J.J. Cole, A. McColl, R. Shaw, M.E. Lynall, P.J. Cowen, P. de Boer, et al., No evidence for differential gene expression in major depressive disorder PBMCs, but robust evidence of elevated biological ageing, Transl. Psychiatry 11 (1) (2021) 11, https://doi.org/10.1038/s41398-021-01506-4.

[40] D. Szklarczyk, A.L. Gable, K.C. Nastou, D. Lyon, R. Kirsch, S. Pyysalo, et al., The STRING database in 2021: customizable protein-protein networks, and functional characterization of user-uploaded gene/measurement sets (vol 49, pg D605, 2021), Nucleic Acids Res. 49 (18) (2021) 10800, https://doi.org/10.1093/nar/gkaa1074.

[41] M. Amir Siddiqui, Akhtar J. Badruddeen, et al., Chrysin modulates protein kinase IKKε/TBK1, insulin sensitivity and hepatic fatty infiltration in diet-induced obese mice, Drug Dev. Res. 83 (1) (2022) 194–207, https://doi.org/10.1002/ddr.21859.

[42] C.Y. Wang, J.K. Liao, A mouse model of diet-induced obesity and insulin resistance, Methods Mol. Biol. 821 (2012) 421–433, https://doi.org/10.1007/978-1-61779-430-8_27.

[43] W. Liu, W.X. Li, Z.K. Wang, Y. Zhu, D.W. Ye, G.M. Zhang, Metabolically abnormal obesity increases the risk of advanced prostate cancer in Chinese patients undergoing radical prostatectomy, Cancer Manag. Res. 12 (2020) 1779–1786, https://doi.org/10.2147/cmar.s242193.

[44] M.T. Tsou, C.H. Yun, J.L. Lin, K.T. Sung, J.P. Tsai, W.H. Huang, et al., Visceral adiposity, pro-inflammatory signaling and vasculopathy in metabolically unhealthy non-obesity phenotype, Diagnostics 11 (1) (2021) 16, https://doi.org/10.3390/diagnostics11010040.

[45] G.I. Smith, B. Mittendorfer, S. Klein, Metabolically healthy obesity: facts and fantasies, J. Clin. Invest. 129 (10) (2019) 3978–3989, https://doi.org/10.1172/jci129186.

[46] G.A. Bray, C. Bouchard, The biology of human overfeeding: a systematic review, Obes. Rev. 21 (9) (2020) 78, https://doi.org/10.1111/obr.13040.

[47] H. Choi, H. Lim, Y.S. Kim, S.Y. Rhee, J.E. Yim, Differences of regional fat distribution measured by magnetic resonance imaging according to obese phenotype in Koreans, Metab. Syndr. Relat. Disord. 20 (10) (2022) 551–557, https://doi.org/10.1089/met.2022.0044.

[48] J.C. Ding, X.J. Chen, Z. Shi, K.Z. Bai, S.H. Shi, Association of metabolically healthy obesity and risk of cardiovascular disease among adults in China: a retrospective cohort study, Diabetes Metab Syndr Obes 16 (2023) 9, https://doi.org/10.2147/dmso.s397243.

[49] Y. Zhou, X. Zhang, L. Zhang, et al., Increased stroke risk in metabolically abnormal normal weight: a 10-year follow-up of 102,037 participants in China, Transl Stroke Res 12 (5) (2021) 725–734, https://doi.org/10.1007/s12975-020-00866-1.

[50] W.X. Xu, J. Zhang, Y.T. Hua, S.J. Yang, D.D. Wang, J.H. Tang, An integrative pan-cancer analysis revealing LCN2 as an oncogenic immune protein in tumor microenvironment, Front. Oncol. 10 (2020) 11, https://doi.org/10.3389/fonc.2020.605097.

[51] N. Hu, C.Y. Chen, J.H. Wang, J. Huang, D.H. Yao, C.L. Li, Atorvastatin ester regulates lipid metabolism in hyperlipidemia rats via the PPAR-signaling pathway and HMGCR expression in the liver, Int. J. Mol. Sci. 22 (20) (2021) 19, https://doi.org/10.3390/ijms222011107.

[52] C.X. Cao, R.N. Wu, X.Y. Zhu, Y. Li, M. Li, F.Y. An, et al., Ameliorative effect of Lactobacillus plantarum WW-fermented soy extract on rat fatty liver via the PPAR signaling pathway, J. Funct.Foods 60 (2019) 9, https://doi.org/10.1016/j.jff.2019.103439.

[53] A. Rezaeian, M. Karimian, A. Hossienzadeh Colagar, Methylation status of MTHFR promoter and oligozoospermia risk: an epigenetic study and in silico analysis, Cell J 22 (4) (2021) 482–490, 10.22074%2Fcellj.2021.6498.

[54] S. Ahmar, D. Gruszka, In-silico study of brassinosteroid signaling genes in rice provides insight into mechanisms which regulate their expression, Front. Genet. 13 (2022) 22, https://doi.org/10.3389/fgene.2022.953458.

[55] F. Hamde, H. Dinka, M. Naimuddin, In silico analysis of promoter regions to identify regulatory elements in TetR family transcriptional regulatory genes of Mycobacterium colombiense CECT 3035, J. Genet. Eng. Biotechnol. 20 (1) (2022) 12, https://doi.org/10.1186/s43141-022-00331-6.

[56] A. Sloutskin, H. Shir-Shapira, R.N. Freiman, T. Juven-Gershon, The core promoter is a regulatory hub for developmental gene expression, Front. Cell Dev. Biol. 9 (2021) 11, 10.3389%2Ffcell.2021.666508.

[57] K. Bartold, A. Pietrzyk-Le, W. Lisowski, K. Golebiewska, A. Siklitskaya, P. Borowicz, et al., Promoting bioanalytical concepts in genetics: a TATA box molecularly imprinted polymer as a small isolated fragment of the DNA damage repairing system, Mater. Sci. Eng., C 100 (2019) 1–10, https://doi.org/10.1016/j.msec.2019.02.038.

[58] A.L. McCleary-Wheeler, B.D. Paradise, L.L. Almada, A.J. Carlson, D.L. Marks, A. Vrabel, et al., TFII-I-mediated polymerase pausing antagonizes GLI2 induction by TGFβ, Nucleic Acids Res. 48 (13) (2020) 7169–7181, 10.1093%2Fnar%2Fgkaa476.

[59] M.A.I. Al-Obaide, K.S. Srivenugopal, Transcriptional pausing and activation at exons-1 and-2, respectively, mediate the "MGMT" gene expression in human glioblastoma cells, Genes 12 (6) (2021) 15, https://doi.org/10.3390/genes12060888.

[60] P.C. FitzGerald, D. Sturgill, A. Shyakhtenko, B. Oliver, C. Vinson, Comparative genomics of Drosophila and human core promoters, Genome Biol. 7 (7) (2006) 22, https://doi.org/10.1186/gb-2006-7-7-r53.

[61] U. Ohler, D.A. Wassarman, Promoting developmental transcription, Development 137 (1) (2010) 15–26, 10.1242%2Fdev.035493.

[62] P. Scalia, S.J. Williams, A. Giordano, Core element cloning, cis-element mapping and serum regulation of the human EphB4 promoter: a novel TATA-less Inr/MTE/DPE-like regulated gene, Genes 10 (12) (2019) 9, https://doi.org/10.3390/genes10120997.

[63] D. Takai, P.A. Jones, Comprehensive analysis of CpG islands in human chromosomes 21 and 22, Proc. Natl. Acad. Sci. U.S.A. 99 (6) (2002) 3740–3745, https://doi.org/10.1073/pnas.052410099.

[64] N. Murugan, R. Kumar, S.K. Pandey, P. Dhansu, M. Chennappa, S. Nallusamy, et al., In silico dissection of regulatory regions of PHT genes from saccharum spp. hybrid and sorghum bicolor and expression analysis of PHT promoters under osmotic stress conditions in tobacco, Sustainability 15 (2) (2023) 17, https://doi.org/10.3390/su15021048.

[65] J.A. Beshir, M. Kebede, In silico analysis of promoter regions and regulatory elements (motifs and CpG islands) of the genes encoding for alcohol production in Saccharomyces cerevisiaea S288C and Schizosaccharomyces pombe 972h, J. Genet. Eng. Biotechnol. 19 (1) (2021) 14, https://doi.org/10.1186/s43141-020-00097-9.

[66] H. Si, T. Gao, J. Yang, et al., Multi-omics reveals hypertrophy of adipose tissue and lipid metabolism disorder via mitochondria in young mice under real-ambient exposure to air pollution, Front. Pharmacol. 14 (2023) 1122615, https://doi.org/10.3389/fphar.2023.1122615.

[67] T. Später, J.E. Marschall, L.K. Brücker, et al., Vascularization of microvascular fragment isolates from visceral and subcutaneous adipose tissue of mice, Tissue Eng Regen Med 19 (1) (2022) 161–175, https://doi.org/10.1007/s13770-021-00391-8.

[68] B. Mittal, Subcutaneous adipose tissue & visceral adipose tissue, Indian J. Med. Res. 149 (5) (2019) 571–573, https://doi.org/10.4103/ijmr.IJMR_1910_18.

[69] B.R. Freedman, D.J. Mooney, Biomaterials to mimic and heal connective tissues, Adv. Mater. 31 (19) (2019) e1806695, https://doi.org/10.1002/adma.201806695.

[70] X. Qian, X. Meng, S. Zhang, W. Zeng, Neuroimmune regulation of white adipose tissues, FEBS J. 289 (24) (2022) 7830–7853, https://doi.org/10.1111/febs.16213.

[71] S.J. Kim, Y. Choi, Y.H. Choi, T. Park, Obesity activates toll-like receptor-mediated proinflammatory signaling cascades in the adipose tissue of mice, J. Nutr. Biochem. 23 (2) (2012) 113–122, https://doi.org/10.1016/j.jnutbio.2010.10.012.

[72] J.S. Marshall, R. Warrington, W. Watson, H.L. Kim, An introduction to immunology and immunopathology, Allergy Asthma Clin. Immunol. 14 (Suppl 2) (2018) 49, https://doi.org/10.1186/s13223-018-0278-1. Published 2018 Sep. 12.

[73] T. Okada, T. Iwayama, S. Murakami, M. Torimura, T. Ogura, Nanoscale observation of PM2.5 incorporated into mammalian cells using scanning electron-assisted dielectric microscope, Sci. Rep. 11 (1) (2021) 228, https://doi.org/10.1038/s41598-020-80546-0.

[74] J.W. Ballard, N.A. Youngson, Review: can diet influence the selective advantage of mitochondrial DNA haplotypes? Biosci. Rep. 35 (6) (2015) e00277 https://doi.org/10.1042/BSR20150232.

[75] Y. Chen, Z. Zhou, W. Min, Mitochondria, oxidative stress and innate immunity, Front. Physiol. 9 (2018) 1487, https://doi.org/10.3389/fphys.2018.01487.

[76] T. Kawai, M.V. Autieri, R. Scalia, Adipose tissue inflammation and metabolic dysfunction in obesity, Am. J. Physiol. Cell Physiol. 320 (3) (2021) C375–C391, https://doi.org/10.1152/ajpcell.00379.2020.

[77] S. Rome, A. Blandin, S. Le Lay, Adipocyte-derived extracellular vesicles: state of the art, Int. J. Mol. Sci. 22 (4) (2021) 1788, https://doi.org/10.3390/ijms22041788.

[78] C.L. Yen, W.C. Chao, C.H. Wu, et al., Phosphorylation of glycogen synthase kinase-3β in metabolically abnormal obesity affects immune stimulation-induced cytokine production, Int. J. Obes. 39 (2) (2015) 270–278, https://doi.org/10.1038/ijo.2014.93.

[79] P. Su, Y.C. Hsu, Yf Cheng, et al., Strong association between metabolically-abnormal obesity and gallstone disease in adults under 50 years, BMC Gastroenterol. 19 (2019) 117, https://doi.org/10.1186/s12876-019-1032-y.
[80] Y. Yang, Metabolically healthy obesity and risk of incident chronic kidney disease in a Korean cohort study, Iran. J. Public Health 48 (11) (2019) 2007–2015.
[81] Y. Zhou, X. Zhang, L. Zhang, et al., Increased stroke risk in metabolically abnormal normal weight: a 10-year follow-up of 102,037 participants in China, Transl Stroke Res 12 (5) (2021) 725–734, https://doi.org/10.1007/s12975-020-00866-1.
[82] H.N. Choi, H. Lim, Y.S. Kim, S.Y. Rhee, J.E. Yim, Differences of regional fat distribution measured by magnetic resonance imaging according to obese phenotype in Koreans, Metab. Syndr. Relat. Disord. 20 (10) (2022) 551–557, https://doi.org/10.1089/met.2022.0044.
[83] J. Ding, X. Chen, Z. Shi, K. Bai, S. Shi, Association of metabolically healthy obesity and risk of cardiovascular disease among adults in China: a retrospective cohort study, Diabetes Metab Syndr Obes 16 (2023) 151–159, https://doi.org/10.2147/DMSO.S397243.
[84] X. Duan, L. Zheng, X. Zhang, et al., A membrane-free liver-gut-on-chip platform for the assessment on dysregulated mechanisms of cholesterol and bile acid metabolism induced by PM2.5, ACS Sens. 5 (11) (2020) 3483–3492, https://doi.org/10.1021/acssensors.0c01524.
[85] R. Li, Q. Sun, S.M. Lam, et al., Sex-dependent effects of ambient PM2.5 pollution on insulin sensitivity and hepatic lipid metabolism in mice, Part. Fibre Toxicol. 17 (1) (2020) 14, https://doi.org/10.1186/s12989-020-00343-5.
[86] Z. Liao, J. Nie, P. Sun, The impact of particulate matter (PM2.5) on skin barrier revealed by transcriptome analysis: focusing on cholesterol metabolism, Toxicol Rep 7 (2019) 1–9, https://doi.org/10.1016/j.toxrep.2019.11.014.
[87] Li J, Xiao X, Wang P, et al. PM2.5 Exposure and Maternal Glucose Metabolism in Early Pregnancy: Associations and Potential Mediation of 25-hydroxyvitamin *D. Ecotoxicol Environ Saf*. https://doi.org/10.1016/j.ecoenv.2021.112645.
[88] Z. Li, F. Tian, H. Ban, et al., Energy metabolism disorders and oxidative stress in the SH-SY5Y cells following PM2.5 air pollution exposure, Toxicol. Lett. 369 (2022) 25–33, https://doi.org/10.1016/j.toxlet.2022.08.008.
[89] N. Kang, R. Wu, W. Liao, et al., Association of long-term exposure to PM2.5 constituents with glucose metabolism in Chinese rural population, Sci. Total Environ. 859 (Pt 2) (2023) 160364, https://doi.org/10.1016/j.scitotenv.2022.160364.
[90] Z. Du, L. Lin, Y. Li, et al., Combined exposure to PM2.5 and high-fat diet facilitates the hepatic lipid metabolism disorders via ROS/miR-155/PPARγ pathway, Free Radic. Biol. Med. 190 (2022) 16–27, https://doi.org/10.1016/j.freeradbiomed.2022.07.024.
[91] S. Dai, Z. Wang, Y. Yang, P. Du, X. Li, PM2.5 induced weight loss of mice through altering the intestinal microenvironment: mucus barrier, gut microbiota, and metabolic profiling, J. Hazard Mater. 431 (2022) 128653, https://doi.org/10.1016/j.jhazmat.2022.128653.
[92] S. Chen, M. Li, R. Zhang, et al., Type 1 diabetes and diet-induced obesity predispose C57BL/6J mice to PM2.5-induced lung injury: a comparative study, Part. Fibre Toxicol. 20 (1) (2023) 10, https://doi.org/10.1186/s12989-023-00526-w.
[93] L.C. Costa-Beber, P.B. Goettems-Fiorin, J.B. Dos Santos, et al., Air pollution combined with high-fat feeding aggravates metabolic and cardiovascular diseases: a dangerous, oxidative, and immune-inflammatory association, Life Sci. 317 (2023) 121468, https://doi.org/10.1016/j.lfs.2023.121468.
[94] A. Jiménez-Chávez, R. Morales-Rubio, E. Sánchez-Gasca, et al., Subchronic co-exposure to particulate matter and fructose-rich-diet induces insulin resistance in male Sprague Dawley rats, Environ. Toxicol. Pharmacol. 100 (2023) 104115, https://doi.org/10.1016/j.etap.2023.104115.
[95] O.P. Zordão, C.M. Campolim, V.Y. Yariwake, et al., Maternal exposure to air pollution alters energy balance transiently according to gender and changes gut microbiota, Front. Endocrinol. 14 (2023) 1069243, https://doi.org/10.3389/fendo.2023.1069243.
[96] C.M. Campolim, L. Weissmann, C.K.O. Ferreira, et al., Short-term exposure to air pollution (PM2.5) induces hypothalamic inflammation, and long-term leads to leptin resistance and obesity via Tlr4/Ikbke in mice, Sci. Rep. 10 (1) (2020) 10160, https://doi.org/10.1038/s41598-020-67040-3.
[97] M. Chen, X. Wang, Z. Hu, et al., Programming of mouse obesity by maternal exposure to concentrated ambient fine particles, Part. Fibre Toxicol. 14 (1) (2017) 20, https://doi.org/10.1186/s12989-017-0201-9.
[98] M. Chen, Y. Xu, W. Wang, et al., Paternal exposure to PM2.5 programs offspring's energy homeostasis, Environ. Sci. Technol. 55 (9) (2021) 6097–6106, https://doi.org/10.1021/acs.est.0c08161.
[99] Y. Xu, W. Wang, M. Chen, et al., Developmental programming of obesity by maternal exposure to concentrated ambient PM2.5 is maternally transmitted into the third generation in a mouse model, Part. Fibre Toxicol. 16 (1) (2019) 27, https://doi.org/10.1186/s12989-019-0312-6.
[100] D. Yi, H.P. Nguyen, H.S. Sul, Epigenetic dynamics of the thermogenic gene program of adipocytes, Biochem. J. 477 (6) (2020) 1137–1148, https://doi.org/10.1042/BCJ20190599.
[101] Cennet Yildiz, Mustafa Özilgen, Species-specific biological energy storage and reuse, Energy Storage 4 (6) (2022) e382, https://doi.org/10.1002/est2.382.
[102] E.R. Berger, N.M. Iyengar, Obesity and energy balance considerations in triple-negative breast cancer, Cancer J. 27 (1) (2021) 17–24, https://doi.org/10.1097/PPO.0000000000000502.
[103] N.G. Girer, C.R. Tomlinson, C.J. Elferink, The aryl hydrocarbon receptor in energy balance: the road from dioxin-induced wasting syndrome to combating obesity with ahr ligands, Int. J. Mol. Sci. 22 (1) (2020) 49, https://doi.org/10.3390/ijms22010049.
[104] M.C. Agostin, A.B.M.S. Bassi, Internal energy balances for continuous bodies and systems of particles, ChemTexts 8 (2022) 7, https://doi.org/10.1007/s40828-021-00155-w.
[105] P. Piaggi, Metabolic determinants of weight gain in humans, Obesity 27 (5) (2019) 691–699, https://doi.org/10.1002/oby.22456.
[106] D.S. Ludwig, C.M. Apovian, L.J. Aronne, et al., Competing paradigms of obesity pathogenesis: energy balance versus carbohydrate-insulin models, Eur. J. Clin. Nutr. 76 (9) (2022) 1209–1221, https://doi.org/10.1038/s41430-022-01179-2.
[107] B. Cannon, J.M.A. de Jong, A.W. Fischer, J. Nedergaard, N. Petrovic, Human brown adipose tissue: classical brown rather than brite/beige? Exp. Physiol. 105 (8) (2020) 1191–1200, https://doi.org/10.1113/EP087875.
[108] K.E. Claflin, K.H. Flippo, A.I. Sullivan, et al., Conditional gene targeting using UCP1-Cre mice directly targets the central nervous system beyond thermogenic adipose tissues, Mol. Metabol. 55 (2022) 101405, https://doi.org/10.1016/j.molmet.2021.101405.
[109] J. Baudier, B.J. Gentil, The S100B protein and partners in adipocyte response to cold stress and adaptive thermogenesis: facts, hypotheses, and perspectives, Biomolecules 10 (6) (2020) 843, https://doi.org/10.3390/biom10060843.
[110] G. Grigg, J. Nowack, J.E.P.W. Bicudo, N.C. Bal, H.N. Woodward, R.S. Seymour, Whole-body endothermy: ancient, homologous and widespread among the ancestors of mammals, birds and crocodylians, Biol. Rev. Camb. Phil. Soc. 97 (2) (2022) 766–801, https://doi.org/10.1111/brv.12822.
[111] S.A. Machado, G. Pasquarelli-do-Nascimento, D.S. da Silva, et al., Browning of the white adipose tissue regulation: new insights into nutritional and metabolic relevance in health and diseases, Nutr. Metab. 19 (1) (2022) 61, https://doi.org/10.1186/s12986-022-00694-0.
[112] E.T. Chouchani, L. Kazak, B.M. Spiegelman, New advances in adaptive thermogenesis: UCP1 and beyond, Cell Metabol. 29 (1) (2019) 27–37, https://doi.org/10.1016/j.cmet.2018.11.002.
[113] P. Janovska, P. Zouhar, K. Bardova, et al., Impairment of adrenergically-regulated thermogenesis in brown fat of obesity-resistant mice is compensated by non-shivering thermogenesis in skeletal muscle, Mol. Metabol. 69 (2023) 101683, https://doi.org/10.1016/j.molmet.2023.101683.
[114] Y. Takeda, Y. Harada, T. Yoshikawa, P. Dai, Mitochondrial energy metabolism in the regulation of thermogenic Brown fats and human metabolic diseases, Int. J. Mol. Sci. 24 (2) (2023) 1352, https://doi.org/10.3390/ijms24021352.
[115] Y. Zu, M. Pahlavani, L. Ramalingam, et al., Temperature-dependent effects of eicosapentaenoic acid (EPA) on browning of subcutaneous adipose tissue in UCP1 knockout male mice, Int. J. Mol. Sci. 24 (10) (2023) 8708, https://doi.org/10.3390/ijms24108708.
[116] A.M. Bertholet, Y. Kirichok, Mitochondrial H+ leak and thermogenesis, Annu. Rev. Physiol. 84 (2022) 381–407, https://doi.org/10.1146/annurev-physiol-021119-034405.
[117] D.G. Nicholls, Mitochondrial proton leaks and uncoupling proteins, Biochim. Biophys. Acta Bioenerg. 1862 (7) (2021) 148428, https://doi.org/10.1016/j.bbabio.2021.148428.
[118] K. Lee, Y.J. Seo, J.H. Song, S. Chei, B.Y. Lee, Ginsenoside Rg1 promotes browning by inducing UCP1 expression and mitochondrial activity in 3T3-L1 and subcutaneous white adipocytes, J Ginseng Res. 43 (4) (2019) 589–599, https://doi.org/10.1016/j.jgr.2018.07.005.
[119] H.S. Lee, C.U. Heo, Y.H. Song, K. Lee, C.I. Choi, Naringin promotes fat browning mediated by UCP1 activation via the AMPK signaling pathway in 3T3-L1 adipocytes, Arch Pharm. Res. (Seoul) 46 (3) (2023) 192–205, https://doi.org/10.1007/s12272-023-01432-7.

[120] L. Recinella, B. De Filippis, M.L. Libero, et al., Anti-inflammatory, antioxidant, and WAT/BAT-Conversion stimulation induced by novel PPAR ligands: results from ex vivo and in vitro studies, Pharmaceuticals 16 (3) (2023) 346, https://doi.org/10.3390/ph16030346.
[121] M. Xiao, Y. Zhang, X. Xu, Calorie restriction combined with high-intensity interval training promotes browning of white adipose tissue by activating the PPARγ/PGC-1α/UCP1 pathway, Alternative Ther. Health Med. 29 (3) (2023) 134–139.
[122] J.R. Cook, A.B. Kohan, R.A. Haeusler, An Updated perspective on the dual-track model of enterocyte fat metabolism, J. Lipid Res. 63 (11) (2022) 100278, https://doi.org/10.1016/j.jlr.2022.100278.
[123] W.W. Christie, J.L. Harwood, Oxidation of polyunsaturated fatty acids to produce lipid mediators, Essays Biochem. 64 (3) (2020) 401–421, https://doi.org/10.1042/EBC20190082.
[124] L. Della Guardia, A.C. Shin, White and brown adipose tissue functionality is impaired by fine particulate matter (PM2.5) exposure [published correction appears in J Mol Med (Berl), J. Mol. Med. (Berl.) 100 (5) (2022) 665–676, https://doi.org/10.1007/s00109-022-02183-6, 2022 Apr 27.
[125] M. Riediker, D. Zink, W. Kreyling, et al., Particle toxicology and health - where are we? 16 (1) (2019) 19, https://doi.org/10.1186/s12989-019-0302-8 [published correction appears in Part Fibre Toxicol. 2019 Jun 27;16(1):26]. *Part Fibre Toxicol.*
[126] G. Anvari, E. Bellas, Hypoxia induces stress fiber formation in adipocytes in the early stage of obesity, Sci. Rep. 11 (1) (2021) 21473, https://doi.org/10.1038/s41598-021-00335-1.
[127] D. Malfacini, A. Pfeifer, GPCR in adipose tissue function-focus on lipolysis, Biomedicines 11 (2) (2023) 588, https://doi.org/10.3390/biomedicines11020588.
[128] W.S. Lian, R.W. Wu, Y.S. Chen, et al., MicroRNA-29a in osteoblasts represses high-fat diet-mediated osteoporosis and body adiposis through targeting leptin, Int. J. Mol. Sci. 22 (17) (2021) 9135, https://doi.org/10.3390/ijms22179135.
[129] M. Valko, C.J. Rhodes, J. Moncol, M. Izakovic, M. Mazur, Free radicals, metals and antioxidants in oxidative stress-induced cancer, Chem. Biol. Interact. 160 (1) (2006) 1–40, https://doi.org/10.1016/j.cbi.2005.12.009.
[130] M. Pardo, X. Qiu, R. Zimmermann, Y. Rudich, Particulate matter toxicity is Nrf2 and mitochondria dependent: the roles of metals and polycyclic aromatic hydrocarbons, Chem. Res. Toxicol. 33 (5) (2020) 1110–1120, https://doi.org/10.1021/acs.chemrestox.0c00007.
[131] J. Qi, G. Jiang, Y. Wan, J. Liu, F. Pi, Nanomaterials-modulated Fenton reactions: strategies, chemodynamic therapy and future trends, J. Chem. Eng. 466 (2023) 142960, https://doi.org/10.1016/j.cej.2023.142960, 2023.
[132] J.Q. Lu, C.M.F. Monaco, T.J. Hawke, C. Yan, M.A. Tarnopolsky, Increased intra-mitochondrial lipofuscin aggregates with spherical dense body formation in mitochondrial myopathy, J. Neurol. Sci. 413 (2020) 116816, https://doi.org/10.1016/j.jns.2020.116816.
[133] P. Prasun, I. Ginevic, K. Oishi, Mitochondrial dysfunction in nonalcoholic fatty liver disease and alcohol related liver disease, Transl Gastroenterol Hepatol 6 (2021) 4, https://doi.org/10.21037/tgh-20-125.
[134] S. Miriyala, A.K. Holley, D.K. St Clair, Mitochondrial superoxide dismutase–signals of distinction, Anti Cancer Agents Med. Chem. 11 (2) (2011) 181–190, https://doi.org/10.2174/187152011795255920.
[135] E. Fuentes-Lemus, P. Hägglund, C. López-Alarcón, M.J. Davies, Oxidative crosslinking of peptides and proteins: mechanisms of formation, detection, characterization and quantification, Molecules 27 (1) (2021) 15, https://doi.org/10.3390/molecules27010015.
[136] I. Pérez-Torres, M.E. Soto, V. Castrejón-Tellez, M.E. Rubio-Ruiz, L. Manzano Pech, V. Guarner-Lans, Oxidative, reductive, and nitrosative stress effects on epigenetics and on posttranslational modification of enzymes in cardiometabolic diseases, Oxid. Med. Cell. Longev. 2020 (2020) 8819719, https://doi.org/10.1155/2020/8819719.
[137] C. Lennicke, H.M. Cochemé, Redox metabolism: ROS as specific molecular regulators of cell signaling and function, Mol. Cell 81 (18) (2021) 3691–3707, https://doi.org/10.1016/j.molcel.2021.08.018.
[138] L. Cantini, L. Calzone, L. Martignetti, et al., Classification of gene signatures for their information value and functional redundancy, NPJ Syst Biol Appl 4 (2017) 2. https://doi:10.1038/s41540-017-0038-8.
[139] V. Casadella, S. Tahi, National innovation systems in low-income and middle-income countries: Re-evaluation of indicators and lessons for a learning economy in Senegal, J Knowl Econ 14 (2023) 2107–2137, https://doi.org/10.1007/s13132-022-00945-8.
[140] A.A. Oloyede, N. Faruk, N. Noma, E. Tebepah, A.K. Nwaulune, Measuring the impact of the digital economy in developing countries: a systematic review and meta-analysis, Heliyon 9 (7) (2023) e17654. https://doi:10.1016/j.heliyon.2023.e17654.
[141] K. Sielemann, A. Hafner, B. Pucker, The reuse of public datasets in the life sciences: potential risks and rewards, PeerJ 8 (2020) e9954. https://doi:10.7717/peerj.9954.
[142] M. Walzer, D. García-Seisdedos, A. Prakash, et al., Implementing the reuse of public DIA proteomics datasets: from the PRIDE database to Expression Atlas, Sci. Data 9 (2022) 335, https://doi.org/10.1038/s41597-022-01380-9.